Available online at www.sciencedirect.com

ScienceDirect

Procedia Engineering 00 (2015) 000–000

Procedia Engineering

www.elsevier.com/locate/procedia

6th BSME International Conference on Thermal Engineering (ICTE 2014)

Non-Equilibrium Condensing Flow with Swirl in a Supersonic Nozzle

Toshiaki Setoguchi[a], Shigeru Matsuo[b,*], Mohammad Mamun[c], Yusuke Fukushima[d], Norimasa Shiomi[e], Yuhi Matsuno[d], Heuy Dong Kim[f]

[a]*Institute of Ocean Energy, Saga University, 1 Honjo-machi, Saga-shi, Saga 840-8502, Japan*
[b]*Department of Advanced Technology Fusion, Saga University, 1 Honjo-machi, Saga 840-8502, Japan*
[c]*Department of Mechanical Engineering, Bangladesh University of Engineering & Technology, Dhaka 1000, Bangladesh*
[d]*Graduate School of Science & Engineering, Saga University, 1 Honjo-machi, Saga-shi, Saga 840-8502, Japan*
[e]*Department of Mechanical Engineering, Saga University, 1 Honjo-machi, Saga-shi, Saga 840-8502, Japan*
[f]*School of Mechanical Engineering, Andong National University, 388 Song Cheon Dong, Andong 760-749, Korea*

Abstract

Recently, by combining a swirl flow with non-equilibrium condensation phenomena of condensate gas generated in a supersonic flow, a separating and extracting techniques of condensate gas have been developed. This technique can reduce the size of the device itself without the use of chemicals, significant benefits. However, for performance of the separation and extraction and operating principle, there are many unresolved problems and it is necessary to research further in order to improve the efficiency of the equipment. In the present study, by using a non-equilibrium condensation phenomenon of moist air occurred in the supersonic flow in the annular nozzle with a swirl, the possibility of separation of the condensable gas was examined numerically. As a result, with an increase of swirl number, the condensate occurred in the vicinity of the circumference of the annular nozzle compared with the case of no swirl.

Peer-review under responsibility of organizing committee of the 6th BSME International Conference on Thermal Engineering (ICTE 2014).

* Corresponding author. Tel.: +81-952-28-8606; fax: +81-952-28-8687.
E-mail address: matsuo@me.saga-u.ac.jp

Peer-review under responsibility of organizing committee of the 6th BSME International Conference on Thermal Engineering (ICTE 2014).

Keywords: Compressible Flow ; non-equilibrium condensation ; supersonic nozzle ; swirl ; simulation

1. Introduction

Nomenclature

D	diameter (m)
g	condensate mass fraction
p	static pressure (Pa)
S_0	initial degree of supersaturation
S_w	Swirl number
T	temperature (K)
u,v,w	velocity components (m/s)
x, y, z	Cartesian coordinate (m)

Greek symbols

δ^*	displacement thickness (m)
ρ	density (kg/m3)
ν	kinematic viscosity (m2/s)

Subscripts

0	stagnation point

In recent years, we are faced with solution of environmental problems and the sophistication of the energy structure on a global scale. Demand for natural gas of lower CO_2 emissions in such a situation keeps on rising compared to coal and petroleum [1].

The separation and extraction of condensate gas is important for natural gas processing. Recently, a separating and extracting techniques of condensate gas have been developed by combining a swirl flow with non-equilibrium condensation phenomena [2] of condensate gas generated in a supersonic flow [3-4]. This technique can reduce the size of the device itself without the use of chemicals, significant benefits. However, for performance of the separation and extraction and operating principle, there are many unresolved problems and it is necessary to research further in order to improve the efficiency of the equipment.

The purpose in the present study is to investigate the effects of swirl flow on supersonic annular flow with non-equilibrium condensation by numerical simulation. As a result, the effect of the swirl flow on spatial distribution of condensate was shown qualitatively.

2. Experimental work

In order to validate the present computation, an experimental work was conducted. Figure 1(a) shows a schematic diagram of experimental apparatus. A supersonic indraft wind tunnel where the moist air at atmospheric pressure was drawn into a vacuum tank, was used in the present. Figure 1(b) shows details of test section. An annular nozzle is composed of an inner body and an outer nozzle. The outer nozzle is coaxial with the inner body. Throat diameter of outer nozzle in case without inner body is D = 30 mm and design Mach number at exit in the annular nozzle is 3.0. The pressure measurements were conducted by a pressure transducer (Kulite XT-190) mounted on the pressure holes (diameter : 1.0 mm) along the outer wall.

The supersonic steady flow lasting about 30 seconds was obtained in the test section. The stagnation pressure p_0 of moist air in the reservoir is 99.8 kPa, and the stagnation temperature T_0 is set at 300 K. The values of initial degree of supersaturation S_0, which is the ratio of vapor pressure to the equilibrium saturation pressure corresponding to the inlet temperature, are 0.20 and 0.70.

3. Numerical method

Assumptions of the two phase flow are as follows ; both velocity slip and temperature difference do not exist between condensate particles and gas mixture, and the effect of the condensate particles on pressure is neglected.

The governing equations used in the present study are the 3D compressible Navier-Stokes equations combined with equations of continuity, energy, turbulent kinetic energy, specific dissipation rate, conservation of mass of the liquid phase and conservation of the number density of droplets. To estimate the eddy viscosity, k-ω model was employed in computations [5].

Equation was discretized in space using a cell-centered finite volume formulation with a quadrilateral structured cell system and in time using the Euler implicit method [6]. Furthermore, a third-order accurate MUSCL TVD schemes based on Roe's approximate Riemann solver [7] was applied to the inviscid fluxes and the viscous fluxes were evaluated by second-order accurate central differences method. Generation terms associated with turbulence and condensation were evaluated by first-order accurate central differences method. Unfactored implicit equations derived with no approximate factorization were solved by a point Gauss-Seidel relaxation method [8].

4. Computational conditions

Figure 2 shows a computational domain of the supersonic annular flow field and boundary condition. An annular nozzle used in this calculation is composed of an inner body and an outer nozzle. The outer nozzle is coaxial with the inner body. Throat diameter of the outer nozzle in case without the inner body is D = 10 mm which is the same as one at the nozzle exit. Values of a in Fig.2(b) are 2° and 4°. Design Mach numbers for the nozzles of a =2° and 4° are 1.97 and 2.24, respectively.

Table 1 shows initial conditions used in the present calculation. Stagnation pressure p_0 and temperature T_0 at stagnation point are 101.3 kPa and 300 K, respectively. The initial degree of supersaturation S_0 of moist air is 0.70.

5. Result and discussions

Figure 3 shows static pressure distributions on the outer wall in cases of S_0 = 0.20 (dry air) and 0.70 (moist air), respectively (p_0= 99.8 kPa, T_0= 300 K). In this figure, comparison between the experimental and simulated static pressure distributions is shown and it is found from this figure that simulated results agree well with experimental results qualitatively.

Figures 4(a) and 4(b) show contour maps of condensate mass fraction g in cases of a = 2° and 4°, respectively. As seen from both figures, positions of sonic line and onset of condensation move upstream with an increase of swirl number and this tendency appears particularly in the range close to the inner side significantly.

Figures 5(a) and 5(b) show contour maps of static pressure p/p_0 in cases of a = 2° and 4°, respectively (S_0=0). It is found from these figures that static pressure decreases rapidly from upstream of the annular nozzle with an increase of swirl number. As a result, onset of condensation is considered to move upstream as shown in Fig.4.

Figure 6 shows distributions of static pressure p/p_0 and g along line A-A' for a = 2° (Fig.6(a)) and 4° (Fig.6(b)). As seen clearly from this figure, static pressure becomes small with an increase of swirl number and the position that g begins to increase moves upstream. Further, g for a = 4° increases rapidly compared to the case of a = 2°.

In order to investigate the amount of condensate in the range of the outer side in the annular nozzle, a new function defined by the following equation was introduced.

$$G = \frac{\int_{y_{center}}^{y_{outer}} 2\pi g \rho u r dr}{\int_{y_{inner}}^{y_{outer}} 2\pi g \rho u r dr}$$

where G shows ratio of integrated value of mass flow rate of the liquid phase from centre plane of the channel to outer wall to integrated value of mass flow rate of the liquid phase from inner wall to outer wall in the cross section in the

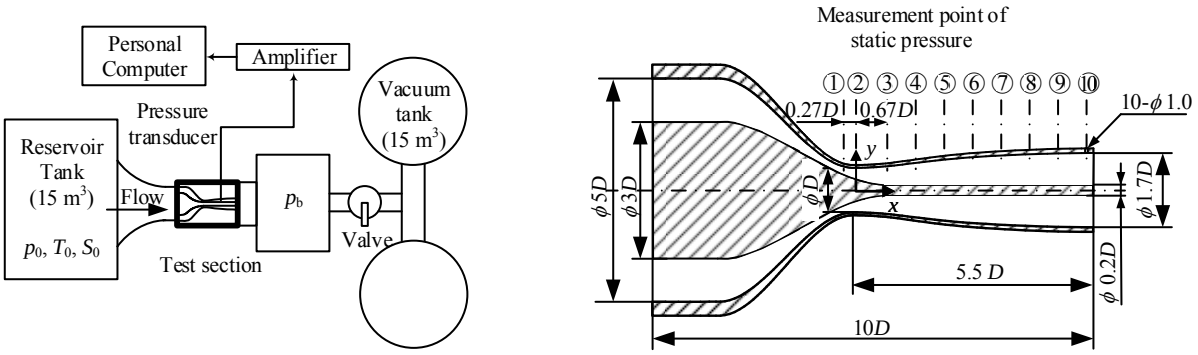

(a) Experimental apparatus (b) Supersonic nozzle with inner body (D = 30 mm)

Fig. 1 Experimental apparatus and supersonic nozzle with inner body geometries

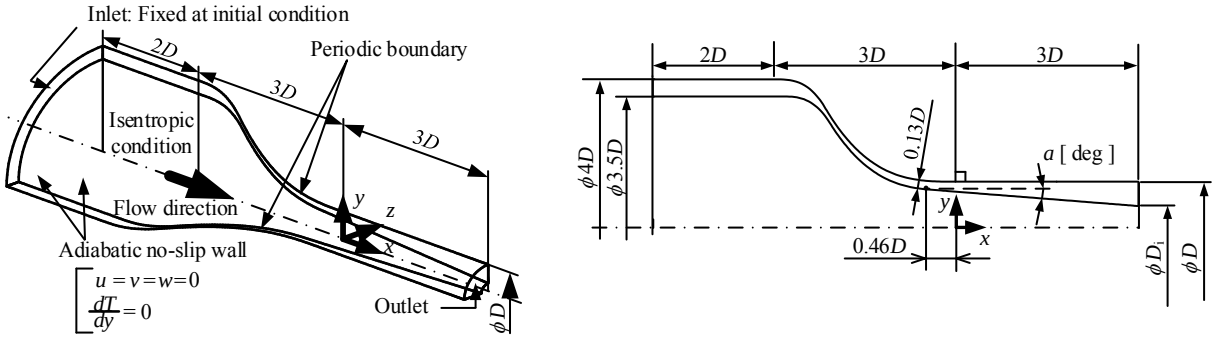

(a) Boundary condition (b) Nozzle details (D = 10 mm, D_i = 0.525D (a = 2°), D_i = 0.287D (a = 4°))

Fig.2 Computational domain and boundary condition

Table 1 Initial conditions

(a) a = 2°

Case	p_0 [kPa]	T_0 [K]	D [mm]	S_0 [-]	S_w [-]
AD-0	101.2	293	10	0.0	0.0
AD-1					1.0
AD-2					2.0
AM-0				0.8	0.0
AM-1					1.0
AM-2					2.0

(b) a = 4°

Case	p_0 [kPa]	T_0 [K]	D [mm]	S_0 [-]	S_w [-]
BD-0	101.2	293	10	0.0	0.0
BD-1					1.0
BD-2					2.0
BM-0				0.8	0.0
BM-1					1.0
BM-2					2.0

annular nozzle channel perpendicular to the x-axis. Figure 7 shows distributions of G along x-axis for a = 2° and 4°. In downstream of the annular nozzle, G in case with swirl becomes large with an increase of swirl number comparison with cases of no swirl (AM-0, BM-0). This means that the condensate gathers toward the outer wall side than cases of no swirl. In particular, in case of a = 4° and S_w=2.0, G becomes the largest.

Figures 8(a) and 8(b) show distributions of displacement thickness of boundary layer δ^* on the inner and outer walls for a = 2° and 4°, respectively (S_0=0). From δ^* in Figs.8(a) and Fig.8(b), it is found that the displacement thickness in the case with swirl becomes thick in the inner side and thin in the outer side comparison with the case without swirl. Further, with an increase of S_w, it becomes thicker in the inner side and thinner in the outer side.

Figures 9(a) and 9(b) show distributions of dynamic viscosity ν on B-B' and C-C' lines in the range close to the inner and outer walls for a = 2° and 4°, respectively (S_0=0). From these figure, the dynamic viscosity of the outer side becomes small and large in the inner side. As a result, it is considered that displacement thickness becomes thin at the outer side and thick in the inner side. Further, it was confirmed that rate of change of density has direct effects on

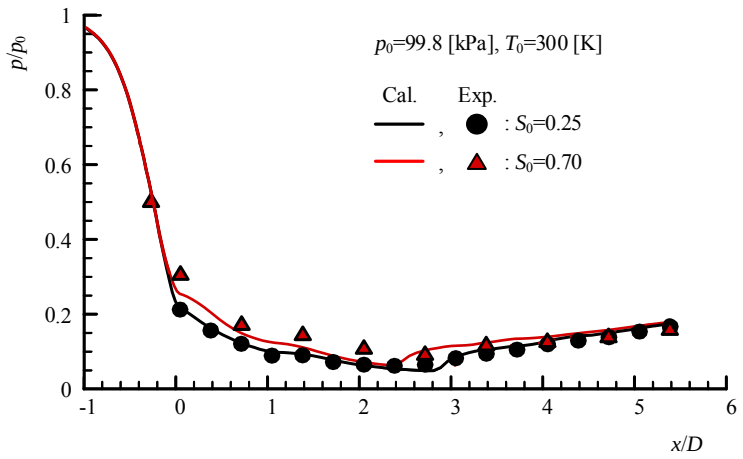

Fig.3 Distributions of static pressure on the outer wall

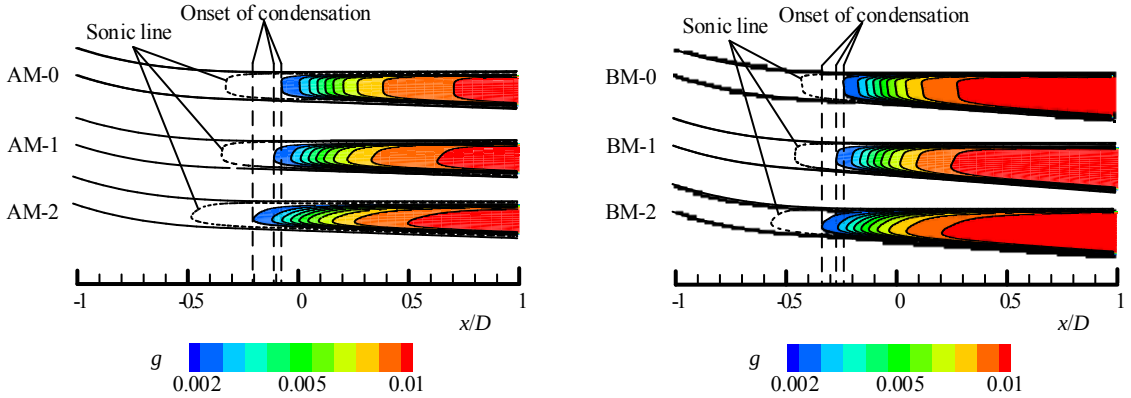

(a) a = 2° (b) a = 4°

Fig.4 Contour maps of g (S_0 = 0)

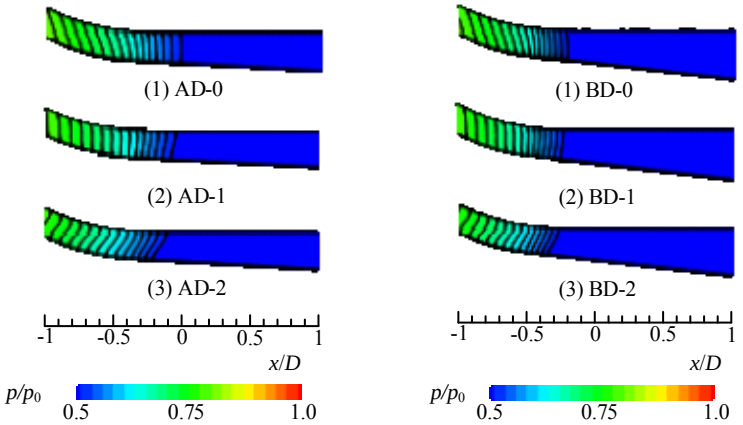

(a) a = 2° (a) a = 4°

Fig.5 Contour maps of static pressure (S_0 = 0)

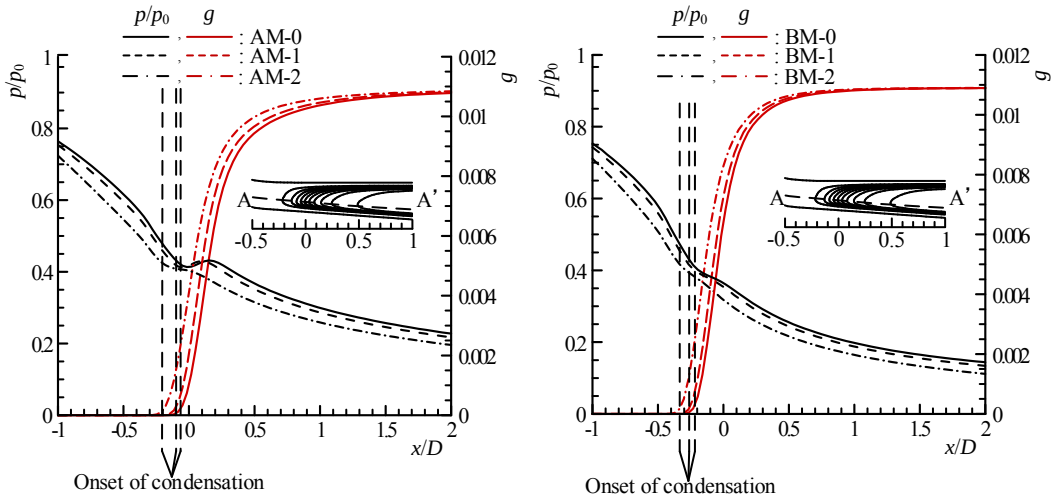

(a) $a = 2°$ (b) $a = 4°$

Fig.6 Distributions of static pressure and g along line A-A'

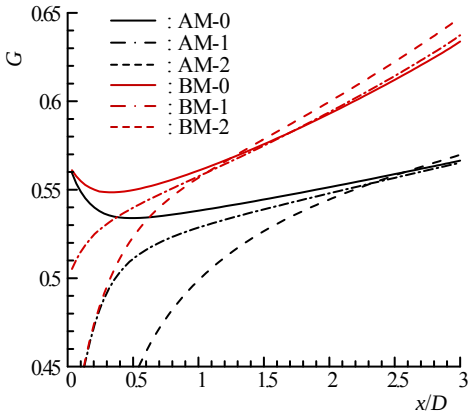

Fig.7 Distributions of G

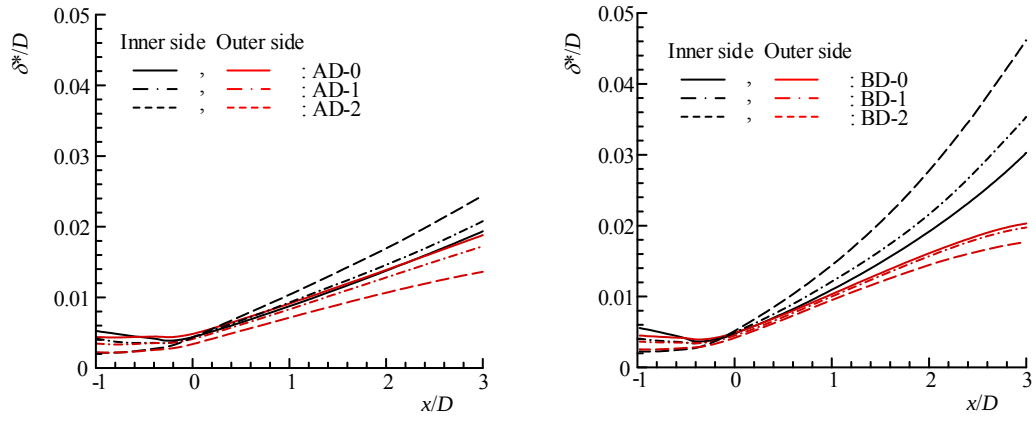

(a) $a = 2°$ (b) $a = 4°$

Fig.8 Distributions of displacement thickness ($S_0 = 0$)

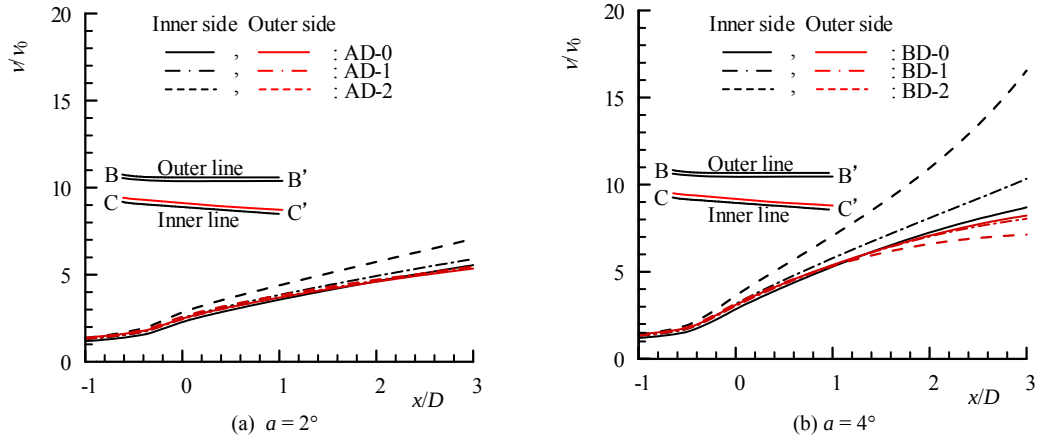

Fig.9 Distributions of ν/ν_0 ($S_0 = 0$)

distributions of ν in comparison with rate of change of viscosity between the case with swirl and the case of no swirl.

For the cause of the distributions of G in Fig.7, it is considered from these results as follows. Non-equilibrium condensation occurs in the range closer to the outer wall in case with swirl because the boundary layer on the outer side becomes thin. On the other hand, the condensation occurs in the range away from the inner wall with comparison to case of no swirl because the boundary layer at the inner side becomes thick.

6. Conclusions

A computational study has been made to investigate the effects of swirl flow on supersonic annular flow with non-equilibrium condensation and spatial distribution of condensate in the annular nozzle was shown qualitatively. The results obtained are as follows:

(1) The positions of sonic line and onset of condensation moved upstream with an increase of swirl number and this tendency appeared particularly in the range close to the inner side significantly.
(2) The displacement thickness of boundary layer in the case with swirl became thick in the inner side and thin in the outer side comparison with the case without swirl.
(3) In downstream of the annular nozzle, mass flow rate of condensate in the range of the outer side from the nozzle center in case with swirl became large in comparison with the case of no swirl and it increased with an increase of swirl number.
(4) Change in dynamic viscosity, particularly density has direct effects on the change in displacement thickness of boundary layer.

Acknowledgements

This work was supported by JSPS KAKENHI Grant Number 26420116. We would like to express our thanks.

References

[1] H. Kaneko, Liquefied petroleum gas supply and demand perspective and LP gas synthesis technology development, 86(4) (2007), pp. 232-237.
[2] P.P. Wegener, L.M. Mach, Condensation in supersonic and hypersonic wind tunnels, Advances in applied mechanics, 5 (1958), pp. 307-447.
[3] B. Prast, B. Lammers, M. Betting, CFD for supersonic gas processing, The 5th international conference on CFD in the process industries (2006), pp.1-6.
[4] C. Wen, X. Cao, Y. Yang, J. Zhang, Evalution of natural gas dehydration in supersonic swirling separators applying the discrete particle method, advanced powder technology, 23(2) (2012), pp. 228-233.
[5] D.C. Wilcox, Formulation of the k-ω turbulence model revisited, AIAA Journal, 46(11) (2008), pp. 2823-2838.

[6] M. Furukawa, T. Nakano, M. Inoue, Unsteady Navier-Stokes simulation of transonic cascade flow using an unfactored implicit upwind relaxation scheme with inner iterations, Transactions of the ASME, Journal of Turbomachinery, 114(3) (1992), pp. 599-606.
[7] P.L. Roe, Approximate Riemann solvers, parameter vectors, and difference schemes, Journal of Computational Physics, 43 (1981), pp. 357-372.
[8] S.P. Chakravarthy, Relaxation methods for unfactored implicit upwind schemes, AIAA paper 84-0165, (1984).

Available online at www.sciencedirect.com

ScienceDirect

Procedia Engineering00 (2015) 000–000

Procedia Engineering

www.elsevier.com/locate/procedia

6th BSME International Conference on Thermal Engineering (ICTE 2014)

Thermodynamic Modeling of Biogas fuelled Automotive Engines

Abhishek Samanta[1], P. C. Roy[2,]*

[1]*Department of Mechanical Engineering, Budge Budge Institute of Technology, Kolkata 700137, India*

[2]*Department of Mechanical Engineering, Jadavpur University, Kolkata 700032, India*

Abstract

Gaseous fuels are getting more importance than that of the liquid fuel due to its clean burning because of homogeneous mixture and large flammability limit. Among the many different types of alternative fuels, biogas from anaerobic digestion of biomass appears to be one of the most promising options. In the present work, a single zone, thermodynamic model of biogas fuelled engine has been developed based on geometrical property, variation of specific heats of gas mixture (air-fuel mixture and combustion products) and chemical equilibrium. Heat transfer loss has been calculated using heat transfer coefficient which is function of pressure, velocity of burned gas, combustion chamber diameter, temperature, along with crank angle. The results from this model have been successfully validated with the experimental results. The effect of spark timing on the engine performance has been optimized and performance parameters have been presented and discussed.

Peer-review under responsibility of organizing committee of the 6th BSMEInternational Conference on Thermal Engineering (ICTE 2014).

Keywords: Alternative fuel; Biogas engine;Gas-mixture model; Engine performance.

1. Introduction

In modern days, there is a need of alternative renewable automotive fuels other than conventional fuel because the conventional fossil fuels are depleting in nature and there is a rapidly rise in price in the international market. Moreover, gaseous fuels are getting more importance other than the liquid fuel due to its clean burning. Gaseous fuel has high hydrogen to carbon ratio which also leads to low carbon dioxide emission. LPG, CNG are petroleum

* Corresponding author. Tel.: +91 3321146890;
*E-mail address:*prokash.roy@gmail.com

1877-7058
Peer-review under responsibility of organizing committee of the 6th BSME International Conference on Thermal Engineering (ICTE 2014).

based gaseous fuel are not renewable energy but hydrogen, biogas, producer gas derived from biomass are renewable in nature. Energy from biomass will be a reliable energy option where there is lack of conventional sources and located far away from the grid and abundant availability of biomass other than wood biomass [1,2]. According to 'National Dairy Development Board India' India had 199.1 million cattle in the year of 2007 that leads to a high potential source of renewable biogas [3]. Lime water scrubber is used to reduce the carbon dioxide and hydrogen sulphide (H_2S) level in biogas [4]. Porpatham [5] investigated the effect of concentration of carbon dioxide in biogas (level from 41% to 30% and 20%) on change of brake power with equivalence ratio, change in cylinder pressure and heat release rate with crank angle in different concentration of methane in biogas. Huang [6] investigated a variable compression ratio Ricardo E6 single cylinder spark ignition engine running on biogas as fuel that the presence of carbon dioxide can improve NOx emission, but in case of low cylinder pressure, engine power and thermal efficiency are reduced and unburned hydro carbon emission is increased. Research work [7] on dual–fuel diesel engine using simulated biogas showed that there is more rapid pressure rise on combustion.

There are two ways of using biogas in an internal combustion engine. The gas can either be used directly in a spark ignition engine, or a compression ignition engine can be employed in a dual fuel mode using liquid pilot fuel. Generally gas engines can be converted to burn treated biogas by (i) modifying carburetion and (ii) adjusting the timing on the spark. Spark ignited gasoline engines may be converted to operate on biogas by changing the carburetor to one that operates on gaseous fuels.

In modeling of the spark ignition engine, heat release calculations for engine, the specific heat ratio is the most important thermodynamic factor. Gatowski [8] had developed a single zone heat release model which is based on the 1st law of thermodynamics. Huffman [9] presented the initiation and duration of heat release for the analysis of the effect of timing on spark and compression ignition engine by combining the ideal gas law with heat release model. Yusaf [10] had developed a single zone engine model to predict the transient heat flux in the time of combustion in a spark ignition engine. Abu Nada [11,12] studied the thermodynamics analysis of spark-ignition engine using single zone model and considered the variation of specific heat named as gas-mixture model.

Nomenclature

A	Area
B	Bore
$\dot{m}$	Mass flow rate
u	Internal energy
P	Pressure
Q	Heat Transfer
θ	Crank angle
Δθ	Duration of Burning
R	Ratio of connecting rod to crank radius length (l/r)
V	Volume
k	Specific heat ratio

Subscripts

g	Gas
l	Loss
w	Wall
f	Fuel

2. Model Descriptions

Model has been developed considering single zone and thermodynamic parameters have been calculated considering the properties each species present in the cylinder during the cycle considering following assumptions

- The cylinder charge (air-fuel mixture) and combustion product mixture are assumed as homogeneous and ideal gas.

- The compression and expansion stroke of engine cycle have been considered neglecting pumping work during suction and exhaust stroke.
- Chemical equilibrium exists among the gaseous species inside the combustion chamber.
- The specific heats of the gaseous species vary with the local temperature.
- Variations in specific heats have been considered with the change in crank rotation due to change in temperature and composition.
- Heat added to the cycle based on the mass fraction of the fuel burnt as a function of crank angle using Weibe function.
- Heat transfer loss is estimated using heat transfer coefficient which is function of pressure, velocity of burned gas, combustion chamber diameter, temperature, along with crank angle
- There is no effect of combustion chamber design.
- Initial pressure at compression stroke is assumed as atmospheric pressure.

The relationship between the cylinder volume and the crank angle is the function of bore, compression ratio, connecting rod length and stroke. Combustion model has been developed based on the conservation principle applied to a combustion chamber as the control volume

The relation from ideal gas law and its differential form,

$$PV = mR_g T \quad \text{and} \quad \frac{dV}{V} + \frac{dP}{P} = \frac{dT}{T} \tag{1}$$

The relation from conservation of energy can be expressed in differential form and applied to a control volume. The equation becomes for net heat release rate is

$$\frac{dQ_n}{d\theta} = mc_v \frac{dT}{d\theta} + P\frac{dV}{d\theta} \tag{2}$$

Rearranging equations (1 and 2)

$$\frac{dP}{d\theta} = \frac{k-1}{V}\frac{dQ_n}{d\theta} - \frac{kP}{V}\frac{dV}{d\theta} \tag{3}$$

The net heat term has both heat added and heat loss in case of combustion

$Q_n = Q_{in} x_b - Q_l$ Where, Q_{in} indicates total heat input and x_b as fraction of heat release,

The heat loss can be obtained as,

$$\frac{dQ_l}{d\theta} = \frac{h_g(\theta) A_w(\theta)}{\omega}(T_w - T_g(\theta)) \tag{4}$$

According to Rakapoulos [12] the temperature of wall can be taken as constant. In the present work the ratio of temperature is taken as

$T_w / T_1 = 1.2$

The mass fraction of fuel burned in an internal combustion engine can be expressed as a function of crank angle using the Wiebe function,

$$x_b(\theta) = 1 - \exp\{-a(\frac{\theta - \theta_s}{\Delta\theta})^n\} \tag{5}$$

Net heat input (Q_{in}) can be expressed as

$$Q_{in} = V_f \eta_v Q_{LHV} \tag{6}$$

Where, V_f is the volume of fuel inside the combustion chamber, η_v is the volumetric efficiency and Q_{LHV} is the lower heating value of fuel.

Hohenberg [14] modified the Woschni [15] correlation to give a better prediction. In the present work heat transfer coefficient by the Woschni model has been used as.

$$h_g(\theta) = 3.26B^{-0.2}P^{0.8}T_g^{-0.55}W^{0.8} \tag{7}$$

Where W is the burned gas velocity.

$W(\theta) = C_1\overline{\vartheta_{pis}} + C_2\frac{V_d T_r}{P_r V_r}[P(\theta) - P_m]$ Here, V_d = displacement volume, P_r, V_r, T_r = are reference state properties at the time of closing inlet valve. P_m = motored pressure (pressure without combustion), and the value of C_1 and C_2 is constant and different for compression and power stroke.

The final relation of combustion chamber pressure with the crank angle is obtained as

$$\frac{dP}{d\theta} = \frac{k-1}{V}[Q_{in}\frac{dx_b}{d\theta} - \frac{h_g(\theta)A_w(\theta)}{\omega}(T_w - T_g(\theta))] - \frac{kP}{V}\frac{dV}{d\theta} \tag{8}$$

The above equation is solved by using explicit finite difference technique with second – order accuracy as [10].

The air fuel mixture is ignited inside of a spark ignition engine. After burning, there is a change in the gas composition occurs with the mass burn fraction (x_b) and equivalence ratio as

$$[Y_1CO_2 + Y_2CH_4] + [\frac{2Y_2}{\phi}](O_2 + 3.76N_2) \rightarrow$$

$$x_b[(2Y_2)H_2O + (Y_1 + Y_2)CO_2] + (1 - x_b)[Y_1CO_2 + Y_2CH_4] + [(2Y_2)(\frac{1}{\phi} - x_b)]O_2 + [3.76(\frac{2Y_2}{\phi})]N_2 \tag{9}$$

Where, Y_i are the mole fraction and $\sum Y_i = 1$, ϕ = equivalence ratio.

In heat release calculation for engine, the specific heat ratio is the most important thermodynamic factor. Gatowski [8] had developed a single zone heat release model which is based on the 1st law of thermodynamics and it is widely used. Klein and Erikson [16] had proposed a specific heat ratio model by using mass burned fraction to calculate the specific heat of burned and unburned mixture. The variation of specific heats of air has been adopted from literature [11]. It was assumed that the air is an ideal gas and the mixture contained 78.1% nitrogen, 20.95% oxygen, 0.92% argon and 0.03% carbon dioxide (molar basis). In practical case, specific heats of all the reactants and the combustion products are temperature dependent. Generally the common combustion products available from biogas fuel are carbon dioxide (CO_2), carbon monoxide (CO), water vapor (H_2O), nitrogen (N_2), oxygen (O_2), hydrogen (H_2) and some of those products have specific heats which is strongly dependent on temperature, while specific heats of other products are less dependent on temperature. So, the most practical approach is to calculate individually the specific heats of reactants and combustion product and then calculate the summation of individual species specific heats. In the present work, the specific heat of clearance volume due to exhaust gas recirculation is also calculated and added with the specific heat of reactant.

The general form of temperature dependent specific heat of a species [17]:

$$\frac{C_p}{R_g} = a_1 + a_2T + a_3T^2 + a_4T^3 \tag{10}$$

Where, a_1 to a_4 are constants, C_p =constant pressure specific heat, R_g =gas constant, T =Temperature of gas mixture.

The molar specific heat is calculated at constant pressure as

$$C_{pmix} = \sum_{i=1}^{n} C_{pi}Y_i \tag{11}$$

C_{pi} are the molar specific heats and Y_i are the mole fraction.

Thus, the specific heat of combustion product can be calculated as

$$C_{p-mix_{product}} = C_{pCO_2}Y_{CO_2} + C_{pCO}Y_{CO} + C_{pH_2O}Y_{H_2O} + C_{pH_2}Y_{H_2} + C_{pO_2}Y_{O_2} + C_{pN_2}Y_{N_2} \quad (12)$$

The specific heat of Clearance volume due to exhaust gas recirculation is calculated as

$$C_{p-clearence-vol} = \sum_{i=1}^{n} V_{ci} \times C_{pi-volumetric} \quad (13)$$

V_{ci} is the individual volume of exhaust gas residue at clearance volume of combustion chamber.

$C_{pi-volumetric}$ is the individual volumetric specific heat of exhaust gas residue.

The specific heat of air-fuel mixture (reactant) can be calculated as

$$C_{p-mix_{reactant}} = C_{pair}Y_{air} + C_{pfuel}Y_{fuel} + C_{p-clearence-vol} \quad (14)$$

During the combustion, it is assumed that the flame front travel throughout the combustion chamber and the gases ahead of the flame are unburned and had the same properties as air-fuel mixture. The gases behind the flame front are assumed burned and it had the properties of combustion product. Thus, the specific heat of the mixture can be calculated as,

$$C_{p-mix} = C_{p-mix_{reactant}} \times (1 - x_b) + C_{p-mix_{product}} \times (x_b) \quad (15)$$

The variation in adiabatic index (k) and the specific heats with crank angle are shown in Fig. 1. It is observed that during the compression stroke the pressure increases inside the combustion chamber as a result the temperature inside the combustion chamber also increases. The value of specific heats increase with the rise in temperature and it leads to a decrease in the value of adiabatic index during the compression stroke. The value of specific heats increases sharply during the combustion process because there is a huge temperature rise during combustion as a result of heat addition. In the expansion process the pressure and temperature decreases gradually as a result value of specific heats also decrease. In this model the ratio of specific heats varies from 1.26 to 1.39 during one crank rotation.

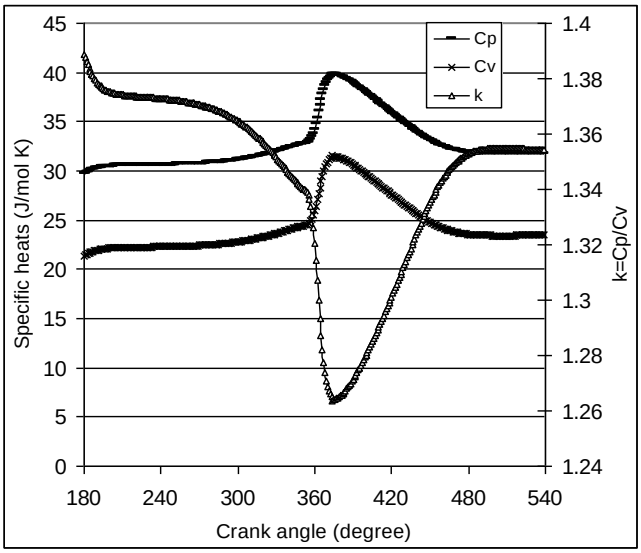

Fig. 1. Variation of specific heats and specific heats ratio along crank angle rotation

In the present work, it is assumed that there are only six species (CO_2, CO, H_2O, N_2, O_2, H_2) in the combustion product. The chemical reaction for combustion can be written as

$$z \cdot CH_4 + w \cdot CO_2 + a \cdot (O_2 + 3.76 \cdot N_2) \rightarrow b \cdot CO_2 + c \cdot CO + d \cdot H_2O + e \cdot H_2 + f \cdot O_2 + g \cdot N_2 \quad (16)$$

Atom balance: $a = (z + 4 \cdot z/4)/\phi$

This chemical reaction is valid for stoichiometric (ϕ =1), rich (ϕ >1) and lean (ϕ <1) mixture. The value of 'b, c, d, e, f, g' denote the number of mole of individual combustion product and value of 'z, w, a' denote the mole number of individual reactant. The solution of six unknowns (b, c, d, e, f, g) require six equations. The balancing of carbon, oxygen, hydrogen and nitrogen atoms provides four equations.

Chemical equilibrium of CO, H_2O, CO_2 and H_2 known as water gas shift reaction has been considered for the combustion. $CO + H_2O \Leftrightarrow CO_2 + H_2$

The equilibrium constant (k_p) of this reaction is temperature dependent, and it also can be calculated from moles of respective species, as:

$$k_p = \frac{b \times e}{d \times c} \tag{17}$$

The equilibrium constant value can be calculated from the change in Gibbs function between the gaseous constituents in the reactants and combustion product at the combustion zone temperature.

$$k_p = \exp\left(-\frac{g^0_{CO_2}}{RT} - \frac{g^0_{H_2}}{RT} + \frac{g^0_{CO}}{RT} + \frac{g^0_{H_2O}}{RT}\right) \tag{18}$$

For Lean fuel-air mixture it is assumed that there is no carbon monoxide (CO) and Hydrogen (H_2) in the combustion product, the number of moles of combustion products are calculated as:

$b = z + w,\ c = 0,\ d = 2,\ e = 0,\ f = a - 2,\ g = 3.76 \times a$

Although, for Rich fuel-air mixture it is assumed that there is no oxygen (O_2) in the combustion product, the number of moles of combustion products are calculated as:

$b = b,\ c = x_1 - b,\ d = -(x_4 + b),\ e = b + x_5,\ f = 0,\ g = 3.76 \times a$

3. Model Validation and Performance Analysis

The model predicted results has been validated with the experimental results reported by Porpatham [5]. The engine specification and operating parameters used in the validation is presented in the Table 1.

Table 1. Engine Specifications and Operating Parameters

Model Engine specifications	
Type	Four stroke, single cylinder, spark ignition engine
Fuel	Biogas, CO2 concentration at 41%,30%,20%
Bore × Stroke	0.0875 × 0.110m
Displacement volume	661.1172 cc
Compression ratio	13:1 (SI version)

3.1 Pressure-Crank Angle Curve Validation:

Typical biogas composition are taken in experiment that was 41%, 30%, 20% carbon dioxide with methane, lime water scrubber is used to reduce the carbon dioxide and hydrogen sulphide (H_2S) level in biogas. Porpatham et al [4] found that the lower heating value increases from 16789 to 28249 kJ/kg when CO_2 concentration reduce from 41% to 20%, when CO_2 concentration is 30% lower heating value is 22951 kJ/kg in full throttle. The value of density of biogas is taken as 0.6797 kg/m³. Model validation have been done in different equivalence ratio as 0.65 as shown in Fig. 2. Different value of parameters a and n of the Weibe function are chosen to fix pressure variation

with crank angle. For different value of a and n pressure versus crank angle curves are also obtained from the model for 20%, 30%, 41% carbon dioxide with methane. These results are compared with the experimental work of Porpatham et al. [5] at equivalence ratio 0.65, the best matches are found at $a = 3.5$, $n = 3.2$ for Biogas with 20% concentration of CO_2, $a = 3.0$, $n = 3.8$ for Biogas with 30% concentration of CO_2, $a = 3.0$, $n = 3.5$ for Biogas with 41% concentration of CO_2.

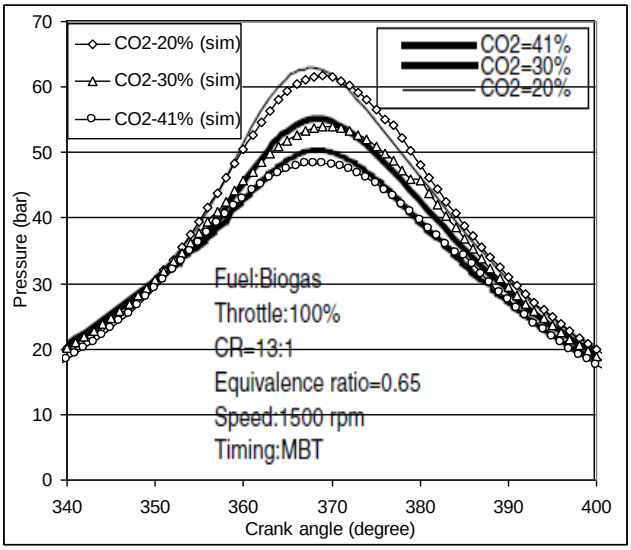

Fig. 2. Variation of cylinder pressure with crank angle at equivalence ratio 0.65 using different % of CO_2 mix

The predicted results correspond well with the experiment results. The rated power of engine is 4.4 kW at 1500rpm at the experimental work of Porpatham et al. [5] and the indicated mean effective pressure is calculated in single zone model as 4.36 bar at 1500 rpm at 20% concentration of CO_2 with biogas. The indicated thermal efficiency is calculated from the model as 26.67%.

3.2 Effect of Variation in Spark Timing

The effect of spark timing in the biogas engine is observed and investigated considering the burning duration at 22° crank angle. Biogas with 20% CO_2 concentration is taken along with equivalence ratio 0.65, a=3.5 and n=3.2, C_1 =0.18, C_2 =0.00324 at power stroke and zero at compression stroke, wall temperature 430K for the analysis. Sparking is done before power stroke and near the end of compression stroke in spark ignition engine. The spark timing is varied from 0° BTDC to 20° BTDC to investigate the effect on biogas engine performance. Fig. 3. shows that the change in peak pressure with crank angle for different spark timing.

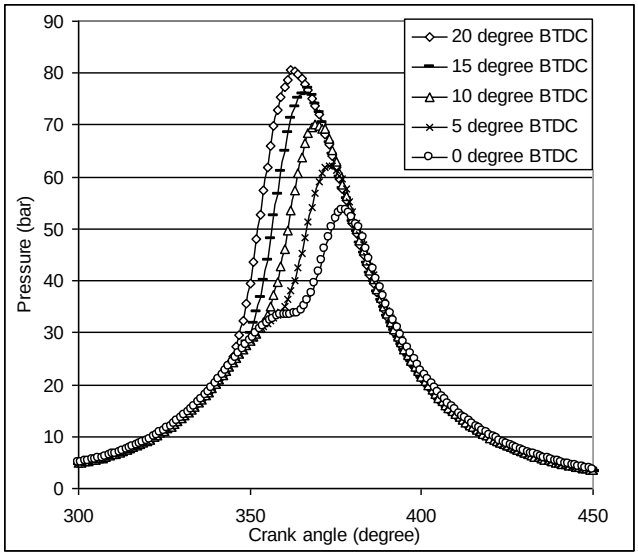

Fig. 3. Effect of spark timing on cylinder pressure

It is observed that at 0° BTDC the total heat release occurs at power stroke and the peak pressure at 19° after TDC so the output work from engine is reduced. The magnitude of peak pressure increases and occurs close to TDC when spark is advanced. In Fig. 3. the peak pressure is almost 1.5 times and occurs after 3° of TDC when the spark occurs at 20° BTDC rather than spark at 0° BTDC. The higher pressure during power stroke increases the positive work generated in power stroke but it also increases the pressure at the end of compression stroke. As a result, more work is consumed in compressing the cylinder charge (air fuel mixture), thus net work from the engine can be maximized for an optimum spark timing.

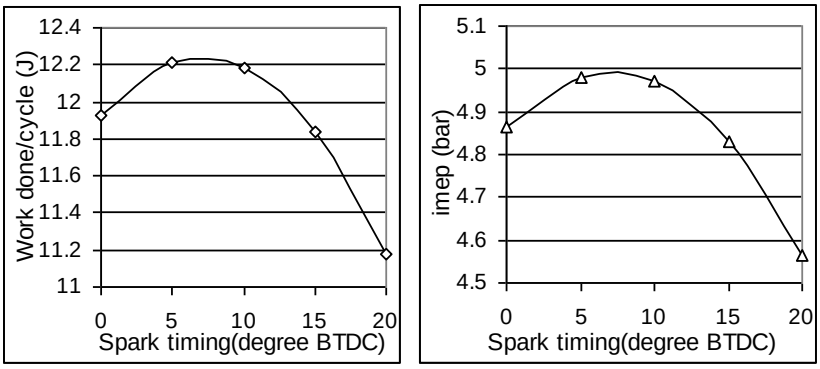

Fig.4.(a) Effect of spark timing on work done per cycle,(b)) Effect of spark timing on indicated mean effective pressure

In Fig. 4. the variation of indicated work done and variation of indicated mean effective pressure (IMEP) with the variation in spark timing is shown. The optimum spark timing which gives maximum indicated work and maximum IMEP is found around at 7° BTDC. The optimum spark location maximizes the indicated thermal efficiency and leads to minimum indicated specific fuel consumption as shown in Fig. 5.

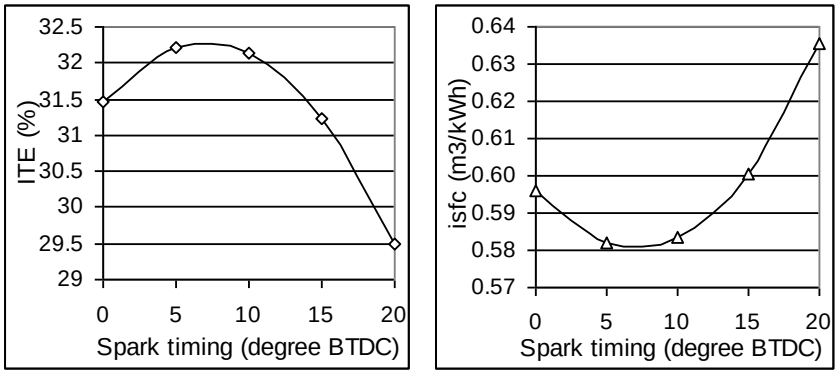

Fig. 5.(a) Effect of spark timing on indicated thermal efficiency (I T E) and (b) Effect of spark timing on indicated specific fuel consumption (isfc)

3.3 Biogas Engine Performance

The biogas engine model has been optimized at burning duration 22° crank angle and for spark timing at 7° BTDC with equivalence ratio 0.65. The lean mixture leads to economical engine performance. In Fig. 6. (a), the variation of pressure and temperature with crank angle are shown. Peak pressure of 66.98 bar is obtained at 12° ATDC (after top dead center) and maximum temperature is obtained at 15° ATDC which is at 1803.14 K.

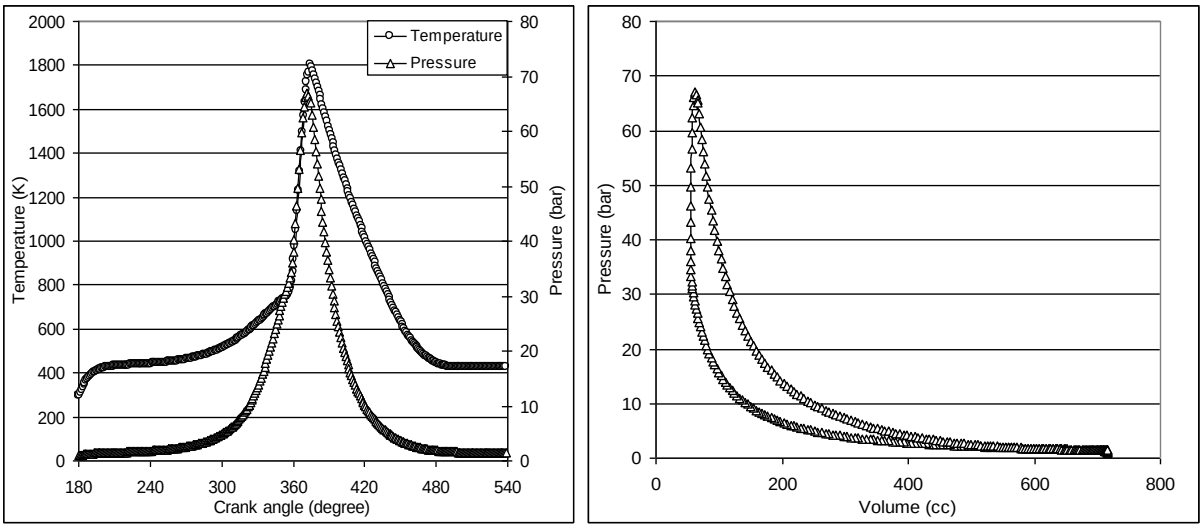

Fig. 6. (a) Temperature and Pressure variation along the crank angle and (b) PV work done per cycle.

Fig. 6. (b) shows the variation in pressure with volume in the combustion chamber. The indicated work is obtained as 13.03 J/cycle and the IMEP is 5.26 bar. Indicated thermal efficiency is calculated as 32.14% and indicated mean specific fuel consumption is 0.583 m^3/kWh.

4. Conclusions

- Single zone thermodynamic model of biogas fired spark ignition and compression ignition engine has been developed using crank-slider model, cylinder pressure model, heat release and heat transfer model.
- A gas mixture model has been introduced to evaluate actual temperature dependent specific heats of reactants and combustion products mixture.
- The biogas fired spark ignition model has been validated with experimental results from literature at different carbon dioxide concentration with biogas. The results from the model correspond well with the experimental results.
- Effect of burning duration and spark timing in spark ignition model have been observed and optimized to obtain maximum indicated work and indicated mean effective pressure for 20% CO_2 concentration with biogas. It has been observed that at burning duration of 22° and 7° BTDC spark timing give the best performance.
- The spark ignition model at optimized condition, the indicated thermal efficiency is calculated as 32.14% and indicated mean specific fuel consumption is 0.583 m^3/kWh.

References

[1]P.C. Roy, Role of Biomass Energy for sustainable development of rural India: case studies. International Journal of Emerging Technology and Advanced Engineering 2013; 3, Special Issue 3: 577-582.

[2]P.C.Roy, A.Datta, N. chakraborty, An assessment of different biomass feedstocks in a downdraft gasifier for engine application. Fuel 2013; 106: 864-868.

[3]National Dairy Development Board India, (2007). Retrieved from National Dairy Development Board India website: http://www.nddb.org/English/Statistics/Pages/Population-India-Species.aspx

[4]S.S. Kapdi, V.K. Vijay, S.K. Rajesh, P. Rajendra, Biogas scrubbing compression and storage perspective and prospectus in India context. International Journal Renewable Energy, 2005; 30:1195–202.

[5]E. Porpatham, A. Ramesh, B. Nagalingam, Investigation on the effect of concentration of methane in biogas when used as a fuel for a spark ignition engine. Fuel, 2008; 87:1651–1659.

[6]J. Huang, R.J. Crookes, Assessment of simulated biogas as a fuel for the spark ignition engine. Fuel, 1998; 77(15):1793–1801

[7]M. M.K. Henham, (1998). Combustion of Simulated Biogas in a Dual-Fuel Diesel Engine. Energy Conversion and Management, 1998; 39(16):2001-2009.

[8]J. A. Gatowski, E.N. Balles, K.M. Chun, F. Nelson, J.A. Ekchian, F.B. Heywood, A heat release analysis of engine pressure data. SAE Paper No: 841359, 1984. DOI: 10.4271/841359.

[9]K. H. Hoffman, S.J. Watowich, R.S. Berry, Optimal paths for thermodynamic systems: the ideal Diesel cycle. J. Appl. Phys, 1985; 58(6): 2125–2134.

[10]T. F. Yusaf, H. Sye, Fong, M.Z. Yusoff, I. Hussein, Modeling of Transient Heat Flux in Spark Ignition EngineDuring Combustion and Comparisons with Experiment. American Journal of Applied Sciences, 2005; 2(10): 1438-1444.

[11]E. Abu Nada, I. Al hinti, A. AlSarkhi, B. Akash, Thermodynamic analysis of spark-ignition engine using a gas mixture model for the working fluid. Int. J. Energy Res, 2007; (31): 1031–1046.

[12]E. Abu Nada, I. Al hinti, A. AlSarkhi, B. Akash, Thermodynamic modeling of spark ignition engine: Effect of temperature dependent specific heats. International Communications in Heat and Mass Transfer, 2006; 33(10): 1264–1272.

[13]C. D. Rakopoulos, Simulation and Analysis of a Natural Aspirated IDI Diesel Engine under Transient Conditions Comprising The Effect of Various Dynamic and Thermodynamic Parameters. Energy Convers. Mgmt, 1998; 39:465-484.

[14]G. F. Hohenberg, Advanced Approaches for Heat Transfer Calculations; SAE Paper 790825, 1979; DOI: 10.4271/790825.

[15]G. Woschni, A Universally Applicable Equation for the Instantaneous Heat Transfer Coefficient in the Internal Combustion Engine, SAE Paper 670931, 1967; DOI: 10.4271/670931.

[16]M. Klein, L. A. Erikson, Specific heat ratio model for single-zone heat release models. SAE Paper No: 2004-01-1464.

[17]C. Ferguson, A. Kirkpatrick, Internal Combustion Engine. Applied Thermosciences. Wiley;New York 2001.

Available online at www.sciencedirect.com

ScienceDirect

Procedia Engineering 00 (2015) 000–000

Procedia Engineering

www.elsevier.com/locate/procedia

6th BSME International Conference on Thermal Engineering (ICTE 2014)

Effects of baffles on flow distribution in an electrostatic precipitator (ESP) of a coal based power plant

A.S.M. Sayem[a]*, M.M.K. Khan[a], M.G. Rasul[a], M.T.O. Amanullah[b], N.M.S. Hassan[a]

[a]*CQUniversity,Rockhampton,Qld-4702, Australia*
[b]*Deakin University,Melborne,Qld-4702, Australia*

Abstract

Electrostatic Precipitators (ESP) are the most reliable and industrially used control devices to capture fine particles for reducing exhaust emission. Its efficiency is 99% or more. However, capturing submicron particles which are hazardous is still a problem as it involves complex flow phenomena and ESP design limitations. In this study, the effect of baffles on flow distribution inside the ESP is investigated computationally. Baffles are expected to increase the residence time of flue gas which helps to collect more particles into the collector plates, and hence increase the collection efficiency of an ESP. Besides, the placement of a baffle is likely to cause swirling of flue gas and hence sub-micron particles move towards the collector plate due to eccentric and electrostatic force. Therefore, the effects of position, shape and thickness of the baffles on collection efficiency which are also important for ESP design are reported in this study. The fluid flow distribution has been modelled using computational fluid dynamics (CFD) software Fluent and the result and outcome are presented and discussed. The result shows that baffles have significant influence on fluid flow pattern and the efficiency of ESP.

Peer-review under responsibility of organizing committee of the 6th BSME International Conference on Thermal Engineering (ICTE 2014).

Keywords: ESP; Flow distribution; residual time; baffles.

1. Introduction

Coal has been a major source of affordable energies for Queensland's electricity generation for decades. In 2010-11, coal based power plant generated around 76 percent of electricity in all over Australia and 62 percent of it was

* Corresponding author. Tel.:+61469378748; fax: +617493 9382.
E-mail address: a.sayem@cqu.edu.au

Peer-review under responsibility of organizing committee of the 6th BSME International Conference on Thermal Engineering (ICTE 2014).

supplied just only to Queensland state and remaining power was supplied to other states [1] which is presented in Fig. 1 . Most of the coal power plants and other process industries generally use Electrostatic Precipitators (ESP) because of their effectiveness and reliability in controlling particulate matters. Before going into the environment, flue gas flows through the ESP where dust particles are captured. The ESP can be used as a cleaning device. For separating the dust particles from the flue gas, an electrical force is generally used by the ESP. A rectangular collection chamber which is known as inlet evase and an outlet convergent duct known as outlet evase are the key components of an ESP. For flow distribution, perforated plates are placed inside the inlet and outlet evase. A number of discharge electrodes (DE) and collection electrodes (CE) are positioned inside the collection chamber. Fig. 2 . presents an ESP arrangement and shows the section of a typical wire-plate ESP channel where a set of discharge electrodes is suspended vertically and the gas flows through this channel. By using an electric field, particle separation is achieved. In this paper the influence of baffles on flow pattern is discussed. Flow pattern has a significant impact on particle collection and is also an important parameter for designing and adjusting the operation of an ESP [2].

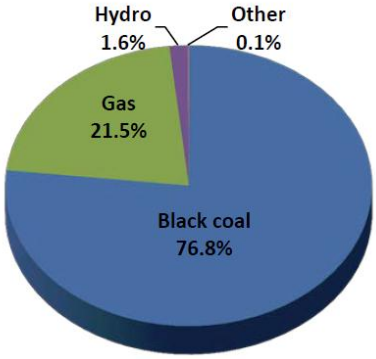

Fig. 1. Queensland grid electricity generations by fuel type, 2010-11 (Source: Electricity gas Australia, 2012)

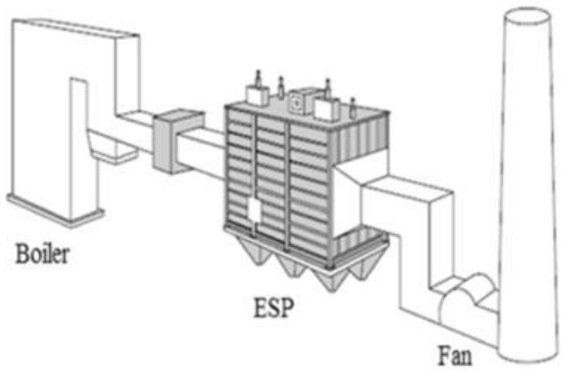

Fig. 2. A typical arrangement of an ESP in the power plant [1]

Particle emissions have become one of the major concerns to power industry because of strict rules and regulations of Environmental Protection Agency (EPA). Particulates contain such materials that can affect our health severely as they may go into the deeper parts of the respiratory tract [3]. Performance optimization of the emission control devices replaces energy recovery and conservation methods. Power stations always desire to control the particulate emissions at a minimum cost in spite of having 99.5% capture capability by the electrostatic

precipitators. Currently, the particles of size particulate matter (PM) 2.5 or less may escape through the ESP. However, it is anticipated that new EPA regulation will soon be imposed for mandatory capture of these particles.

Much work has already been done on the gas flow regime within an ESP in recent years [4]. An overview is described by Gallimberti et al. [5]. It appears that there is a need to further improve ESP's ability and efficiency by capturing these smaller particles. One idea of achieving this is to increase the particle residence time within the ESP. Introduction of column of baffles to increase the residence time of exhaust fluid flow inside the ESP has been considered in this study. Fluid flow which is influenced by vorticity created by the baffles has been examined by a computational fluid dynamics (CFD) analysis.

2. Geometry

A laboratory scale ESP model, geometrically similar to an industrial ESP, was designed and fabricated by Shah et al [4, 6] at the Thermodynamics Laboratory of CQUniversity, Australia to examine the flow behaviour inside the ESP. This laboratory scale ESP consisted of a rectangular collection chamber and an inlet evase and an outlet evase. The current study focuses on further improvement of the flow behaviour inside the ESP and has taken into account the rectangular collection chamber as a rectangular duct for simplicity of the model geometry. This is because the dust particle separation from the flue gas and the collection of dust particles usually occur inside the rectangular duct. The Geometry is drawn in AutoCad 2014 and exported into Fluent for further meshing and refinement. The geometry with dimension is shown in Fig. 3. Rectangular strip is inserted on the wall of the rectangular duct and ANSYS code 'FLUENT' is used for numerical simulation of fluid flow behaviour.

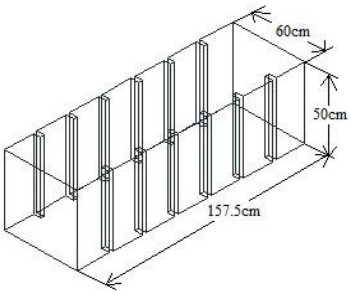

Fig. 3. (a) Duct with baffles.

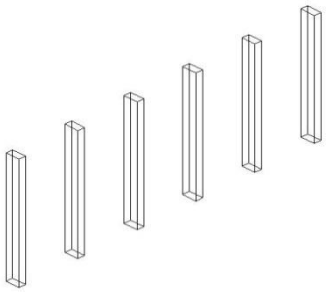

Fig. 3. (b) Inserted baffles.

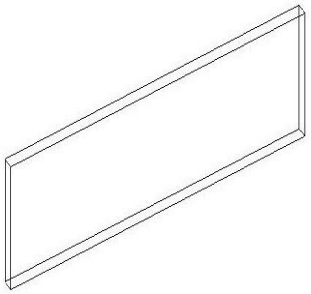

Fig. 3. (c) Side wall.

The ESP considered in this paper has a single chamber. As seen from Fig. 3(a), six rectangular baffles were inserted in two opposite sidewalls. The rectangular baffles and the side wall are shown in Fig. 3(b) and Fig. 3(c) respectively. The length, width and height of the duct are: 157.5 cm, 60 cm and 50 cm respectively. The baffles are equally spaced and the distance between two baffles is 20 cm. The dimension of each baffle is: height 50 cm, width 5 cm and length 2.5 cm.

It is noted that the results of the impact of the baffles on the flow are discussed on a qualitative basis since more results are required for a quantitative analysis.

3. Numerical Approach and Simulation Procedure

As mentioned earlier, the mesh created by Design Modeller is exported to ANSYS to discretize the fluid domain into small cells to form a volume mesh or grid and set up appropriate boundary conditions. Numerical computation

of fluid transport includes continuity, momentum and turbulence model equations. The flow properties and equations are solved and analyzed by CFD code "FLUENT"[7]

Continuity equation:

$$\frac{\partial \bar{u}}{\partial x}+\frac{\partial \bar{v}}{\partial y}+\frac{\partial \bar{w}}{\partial z}=\frac{\partial(u_i)}{\partial x_i}=0 \quad (1)$$

Momentum Equation:

$$\frac{\partial}{\partial t}(\rho u_i)+\frac{\partial}{\partial x_j}(\rho u_i u_j)=-\frac{\partial p}{\partial x_j}+\frac{\partial \tau_{ij}}{\partial x_j}+\rho g_i+F_i \quad (2)$$

In this equation, p is static pressure and self-defined source term are contained in *Fi*, Stress tensor is determined by the following equation:

$$\tau_{ij}=\left[\mu\left(\frac{\partial u_i}{\partial x_j}+\frac{\partial v_j}{\partial x_i}\right)\right]-\frac{2}{3}\mu\frac{\partial u_i}{\partial x_i}\delta_{ij} \quad (3)$$

$$\frac{\partial}{\partial t}(\rho k)+\frac{\partial}{\partial x_j}(\rho k u_j)=\frac{\partial}{\partial x_j}\left[\left(\mu+\frac{\mu t}{\sigma k}\right)\frac{\partial k}{\partial x_j}\right]+(G_k+G_B-Y_M)-\rho\epsilon+S_k \quad (4)$$

$$\frac{\partial}{\partial t}(\rho\epsilon)+\frac{\partial}{\partial x_j}(\rho\epsilon u_i)=\frac{\partial}{\partial x_j}\left[\left(\mu+\frac{u_t}{\sigma\epsilon}\right)\frac{\partial\epsilon}{\partial x_j}\right]+C_{1\epsilon}\frac{\epsilon}{k}(G_k+C_{3\epsilon}G_b)-C_{2\epsilon}\rho\frac{\epsilon^2}{k}+S_\epsilon \quad (5)$$

where u, v, w is each component of gas velocity, (m/s) and μ, μ_t are molecular viscosity and kinetic viscosity (Pa.s) respectively; ρ (kg/m^3) is fluid density, G_k represents turbulent energy generated by mean velocity gradient; G_B is turbulent energy generated by buoyancy; Y_M represents pulsation expansion in turbulent model of compressible flow; $C_{1\epsilon}$, $C_{2\epsilon}$ and $C_{3\epsilon}$ are empirical constant; σk and $\sigma\epsilon$ are corresponding turbulent Prandtl number in k-equation and ε-equation; S_k and S_ε are self-defining source term; $C_{1\epsilon}$ =1.44, $C_{2\epsilon}$ =1.92, $C_{3\epsilon}$=0.09, σk =1.0, $\sigma\epsilon$ =1.3 [8]

Realizable k-ϵ model was selected in this article, as it differs from the others k-ϵ model in two important ways. Firstly, the realizable k-ϵ model contains a new formulation for the turbulent viscosity. Secondly, a new transport equation for the dissipation rate, ε (dissipation rate of turbulent kinetic energy, m^2/s^3), has been derived from an exact equation for the transport of the mean-square velocity fluctuation [7]. The turbulent kinetic energy k (turbulent kinetic energy, m^2/s^2) and its dissipation rate ϵ for Realizable k-ϵ model are obtained from the transport equation (4) and equation (5) respectively [7, 8].

Mesh generation and boundary condition

Three dimensional simplified model of ESP was employed in this study to investigate the flow properties. ANSYS 15.0 was used to establish models for calculating regions where unstructured grids were generated and finally, after resizing and refinement, structured grid was obtained. The number of nodes and cells obtained were 1817424 and 1759268 respectively. Air was used as a fluid and its acquiescent properties were maintained with constant velocity. The boundary conditions were applied as follows: inlet velocity was considered as constant velocity which was 7 m/s, the outlet boundary condition was pressure outlet and "No slip" boundary condition was imposed on the side walls including baffle's side face and front face.

The finite volume methods were used to discretise the partial differential equations of the model. The Semi-Implicit Method for Pressure-Linked Equations (SIMPLE) scheme was used for pressure–velocity coupling and the second order upwind scheme was used because of its combination of accuracy and stability and as this scheme interpolates the variables on the surface of the control volume. Turbulent kinetic energy k and turbulent dissipation rate ε were considered as a second order upwind for better simulation accuracy.

Fig. 4. (a) Structured mesh(3D)

In order to compute the results, all simulations were carried out on an Intel Core i5 processor computer that has 2.80 GHz processor and 8.00 GB of RAM, 64-bit operating system.

4. Results and Analysis

The assembled graphs below are the simulation results of velocity distribution and pressure distribution respectively. Six baffles were inserted into each wall in air flow distribution plates. In the following figures, the influence of baffle on forming skewed air flow pattern is considered only.

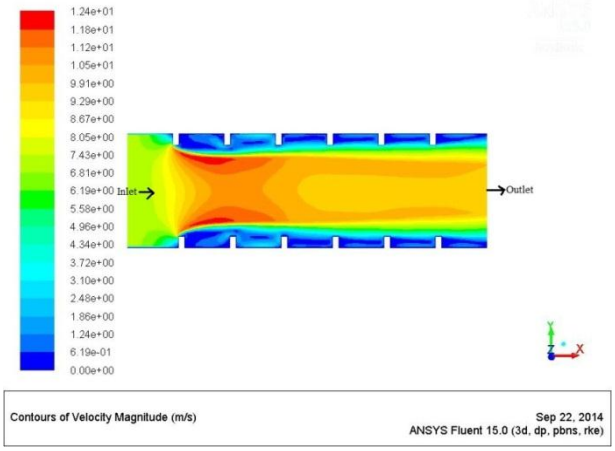

Fig. 5. (a) Contour of velocity magnitude at section x= 150, y= 55 and z= 25

Fig. 5(a) and 5(b) show the contour of the velocity distribution. It is seen from these figures that the velocity keeps increasing towards the center of the channel between the first two baffles with the reduction of flow area. The velocity however gradually decreases near the wall between the two baffles. An irregular skewed flow pattern is formed at the inlet of the first three baffles, however such flow pattern does not continue towards the outlet of the duct. The skewed motion of flue gas is likely to increase the retention time of flue gas inside the duct. From these figures it is observed that near the back face of the baffles, the velocity is small or near zero. This indicates that more dust is likely to settle and accumulate there.

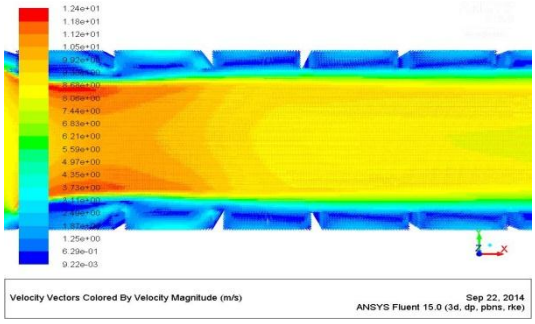

Fig. 5. (b) Contour of velocity vectors

Formation of skewed flow of flue gas in terms of vectors quantity in 3D view is shown in Fig. 5. (b) Fig. 5. (c).As seen the flow propagation is influenced by the skewed flow in the back and gradually the flow becomes steady.

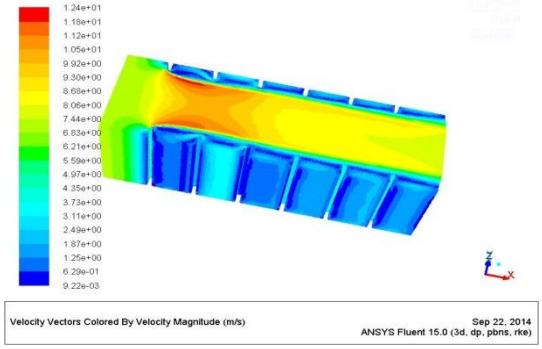

Fig. 5. (c) Contour of velocity vectors in terms of velocity magnitude

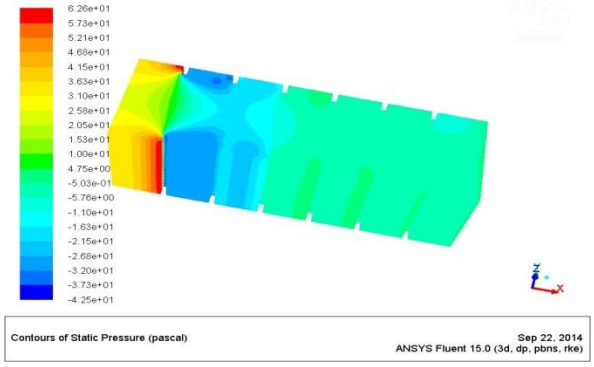

Fig. 5. (d) Contours of Static Pressure

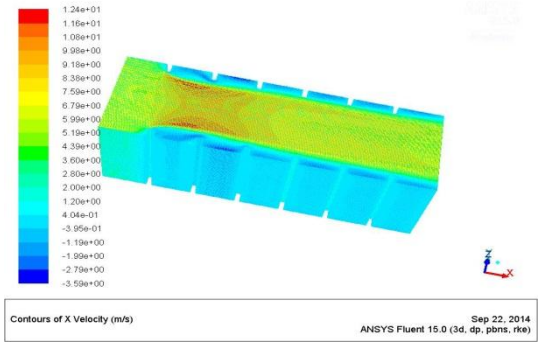

Fig. 5. (e) Contours of X velocity

Fig. 5(d) characterizes the contours of static pressure which shows the creation of a vacuum pressure between first two baffles and Fig. 5 (e) presents the contours of the velocity in the X direction.

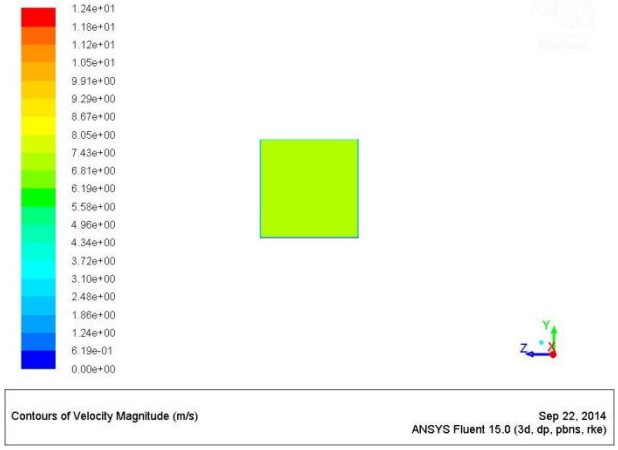

Fig. 5. (f) Inlet velocity

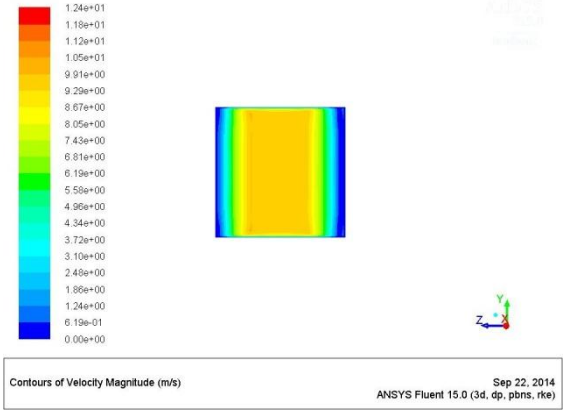

Fig. 5. (g) Outlet velocity

Fig. 5 (f) and Fig. 5(g) represent the contours of inlet velocity and outlet velocity distribution respectively which shows that the velocity at the wall is zero and almost uniform at the inlet. Due to the influence of baffles, the velocity profile at the outlet has changed from that at the inlet which is shown in Fig. 5(g).The blue color zone indicates that the velocity remains zero and small from the side wall up to a certain distance. The zero and small velocity zone on both side walls is suitable for more particle sediment on the side wall.

5. Conclusion and recommendation

The preliminary CFD analysis of this investigation shows some encouraging and favorable results. The conclusions that can be drawn are as below:

- Qualitative analysis of the flow pattern shows that installing baffles makes skewed gas flow whose formation is related to the baffle interval and which also increases the residence time of the flue gas inside the duct leading to more dust collection. Further study will be conducted on changing the baffles angle i.e by inserting the baffles or placing the baffles on an incline inside the duct.

- The dynamics of formation of the skewed flow is complicated and is not quantitatively analysed. However, qualitatively, it shows creation of vortex flow near the baffles and existence of a near zero velocity close to the wall of the baffles, which assists to improve the dust collection efficiency.
- Further investigation needs to be done to determine the strength of vortex flow as this can produce a spinning motion that may wipe out the accumulated dust in the wall.
- It is desirable that the inlet velocity be kept constant and this can be achieved by inserting a porous plate at the inlet. Present study indicates that the inlet air flow is skewed at the entrance point but by varying the number of holes, arrangement and shape of porous plate it can be made more uniform.

References

[1] APTI, Air Pollution Training Institute (APTI) Course SI: 412B. 1998., in, U.S Environmental Protection Agency.,1998.
[2] M. HU, X. SUN, C. MA, Y. and LIU, L.-q. WANG, Numerical Simulation of Influence of Baffler in Electric Field Entrance to Form Skewed Gas Flow.
[3] L. Morawska, V. Agranovski, Z. Ristovski and M. Jamriska, 2002, Effect of face velocity and the nature of aerosol on the collection of submicrometer particles by electrostatic precipitator, Indoor air, 12 (2002) 129-137.
[4] S.M.E. Haque, M.G. Rasul, A.V. Deev, M.M.K. Khan and N. Subaschandar, 2009 Flow simulation in an electrostatic precipitator of a thermal power plant, Applied Thermal Engineering, 29 (2009) 2037-2042.
[5] I. Gallimberti, 1998, Recent advancements in the physical modelling of electrostatic precipitators, Journal of Electrostatics,43 (1998) 219-247.
[6] S.M. Haque, M. Rasul, M.M.K. Khan, A. Deev and N. Subaschandar,2009,Influence of the inlet velocity profiles on the prediction of velocity distribution inside an electrostatic precipitator, Experimental Thermal and Fluid Science, 33 (2009) 322-328.
[7] ANSYS FLUENT 12.0 Theory Guide.
[8] F. Dubois and W. Huamo, 2001, New advances in computational fluid dynamics—theory, methods and applications [M], in,Beijing: Higher Education Press,2001.

Available online at www.sciencedirect.com

ScienceDirect

Procedia Engineering 00 (2015) 000–000

Procedia Engineering

www.elsevier.com/locate/procedia

6th BSME International Conference on Thermal Engineering (ICTE 2014)

Prospect of Underground Coal Gasification in Bangladesh

Mojibul Sajjad [a], Mohammad G. Rasul [b]

[a] *Researcher, School Of Science and Engineering, Central Queensland University, Rockhampton-4702,Australia*
[b] *Associate professor, School of Science and Engineering, Central Queensland University, Rockhampton-4702,Australia*

Abstract

Main source of energy fuel in Bangladesh is natural gas and day by day it is trimming the proven reserves. There are provisions of potential renewable energy resources like the solar, wind, tidal etc.; but the initiatives are very slow. Coal reserves and their prospects could not assure the nation as there are proven coal reserves of about 4,750 Mt (equivalent to 975 GM^3 of gas, which is around 3 times greater than the present gas reserve in Bangladesh). Those coal reserves are discovered in the North-Western part of Bangladesh at the depth ranging 200-1100 m. The special feature of the coal seams are found in the same geological formation and thickness is high (on average 38-64m).One of the major issues, is the minable amount of the resources in conventional mining method. Barapukuria coal mine is under operation since 2005 and running a 250 MW coal fired power plant. But the mining method is not yet proven as suitable one, due to jointed layer thick coal seam (51 m) with faulty overburden and wider aquifer zone. The underground mining environment is hazardous including high temperature, suffocative humidity and releasing of unpredictable carboneus gases from the coal faces which make the life expectancy of this mine questionable. The geographical position and climatic conditions of Bangladesh, especially the monsoon rain extends several weeks to months which are major setback for economic viability of the open striping mining. The policy makers still could not finalize the national coal policy. In this stage the government is stepping up for construction of coal fired power stations run by imported coal. A group of skilled and dedicated entrepreneur is seeking the pathways for exploiting unminable coals within a safe engineering framework and bringing the global Underground Coal Gasification (UCG) projects under the same umbrella. India, Pakistan, Indonesia, Japan even the Vietnam has already joined the cohort. But why not Bangladesh, though they have huge amount of coal reserves which are not minable in conventional methods. This paper presents a review on development of this technology, investigates the geology and formation of the deposits and seeks suitability of the gasification methods as a sustainable engineering model considering social, environmental & economic issues, which may be helpful for fore stepping towards unconventional coal extraction activity for combating energy crisis.

Keywords : Hazardous Coal Mining, Subsidence, Aquifar, Underground Coal Gasification. FEM in ABAQUS, CFD in ANSYS environment.

Peer-review under responsibility of organizing committee of the 6th BSME International Conference on Thermal Engineering (ICTE 2014).

1877-7058
Peer-review under responsibility of organizing committee of the 6th BSME International Conference on Thermal Engineering (ICTE 2014).

1. Introduction

The coals never been treated as prime choice of energy sources because of hazardous & risky extraction procedures as well as environmental pollution. However it is still using as bulk source of energy for electricity generation along with adoption of clean coal technologies (such as Fluidized Bed Combustion, Oxy fuel pre-post combustion etc.) for keeping minimum level of Sulphur, Nitrogen Oxides, Carboneus products at the combustion stages. Another approach named "coal gasification" is adopted for producing synthesis gas from the coal and using as burning fuel or feedstock to chemical products. Underground Coal Gasification (UCG) is a technique, where coal gasifier facilities developed within the coal body itself. Plenty of coal reserves exist in Bangladesh, which are not suitable for extraction through conventional mining. Meeting up the immense energy demand, Bangladesh may consider the UCG for further electricity generation. In this paper we are focusing on prospects of UCG in Bangladesh, later on present a holistic approach for identifying issues to welcome the agencies & business partners.

1.1. What is UCG? Is it a new technology? How is it processed?

UCG (underground coal gasification) has a history of 100 years of efforts & investment; but still is in crippling stage, whereas the technological development has been attained in a mature stage for commercial production. UCG is a self-contained complex thermo-chemical gasification process conducted in situ coal body [1]. This technology originated with German engineer William Siemens in 1860s and later on William Ramsay conducted the successful experiment at Durham coalfield in Northern England [2]. Day by day, many organization, scientists group, countries and regulating bodies are working for establishing this technology as "clean coal" format. The quality of the UCG syngas depends on factors like as; thickness and depth of coal seam, water content, temperature prevails in the gasification cavity, injecting charge (air/ Oxygen). Syngas/ synthetic gas refers to mainly CO-H_2 (carbon monoxide-hydrogen) gas mixture. UCG gas composition will vary depending on the purpose and the geological conditions of the coal reserves. The overall process can be sub divided into mainly (i) Oxidation, (ii) Gasification and (iii) Pyrolysis/de-volatization. For ideal cases the major thermo-chemical reaction processes are described in the Table-1 [3] [4].

Table 1. The reactions involved in coal gasification

Sl.no	Chemical Synthesis	Reaction	Thermodynamic sate
a)	Heterogeneous water gas shift reaction (Exothermic)	$C + H_2O = H_2 + CO$	$\Delta H = +118.5$ kJ /mol
b)	Shift conversion (Endothermic)	$CO + H_2O = H_2 + CO2$	$\Delta H = -42.3$ kJ / mol
c)	Methanation (Endothermic)	$CO+3H_2 = CH_4 + H2O$	$\Delta H = -206.0$ kJ /mol
d)	Hydrogenating gasification (Endothermic)	$C + 2H_2 = CH_4$	$\Delta H = -87.5$ kJ /mol
e)	Partial oxidation (Endothermic)	$C + ½O_2 = CO$	$\Delta H = -123.1$ kJ/ mol
f)	Oxidation (Endothermic)	$C + O_2 = CO_2$	$\Delta H = -406.0$ kJ /mol
g)	Boudouard reaction(Exothermic)	$C + CO_2 = 2CO$	$\Delta H = +159.9$ kJ/ mol

UCG facilities are constructed within the coal seam. A numbers of vertical wells (injection well, production wells, ignition wells etc.) are drilled up to the coal seam and linked up within the coal body through directional drilling/hydraulic fracturing for creating scape way of produced gas through production well. Oxidants (air, oxygen or steam) are injected to ignite and fuelling the underground combustion process. The high pressure (4-10 bar.) combustion is conducted at a temperature of 700–900 °C (1,290–1,650 °F) ; but it may reach up to 1,500 °C (2,730

°F). The process decomposes coal and generates carbon dioxide (CO_2), hydrogen (H_2), carbon monoxide (CO) and small quantities of methane (CH_4) and hydrogen sulphide (H_2S).

1.2 Evolution of UCG Techniques and Modern Practices

UCG is now treated as a composite engineering, where the operators are now capable of predict the availability and reliability of the whole process throughout construction phase, process control & monitor UCG operations along with post operation shut down program. The efficiency of the UCG facilities depends on how the vertical wells are linked to channels for flow of air mixture considering geo-physical property of the coal body and their surroundings. Former Soviet Union (FSU) had established commercial plants and designed linking patterns for gasification chambers depending on coal geology, dip angle of the seam, forward/counter current direction of injected air flow, flow pattern of the product gas towards production well etc. The implementation of the oil & gas technology along with computation methods, remote sensing and data acquisition facilities contributed for up gradation of this industry.

There are various methods for linking the wells such as LVW (linked vertical wells) through hydraulic fracturing, horizontal drilling, reverse combustion, electrical-linkage etc. Controlled Retractable Injection Point (CRIP) method (developed by Lawrence Livermore National Laboratory, USA in1970) is proven techniques where the wells are inter-connected by directional drilling through the coal seam. Coiled tubing burns through the horizontal tunnel borehole casing, oxygen and steam are forced through the point to ignite the coal. The movable injection point begins the burn near the production well. When the first burn expires, a second burn is initiated closer to the injection well. This procedure continues until the seam is burned out. The CRIP process retracts the combined steam and oxygen injection point to control the location of the combustion front[1, 5] .

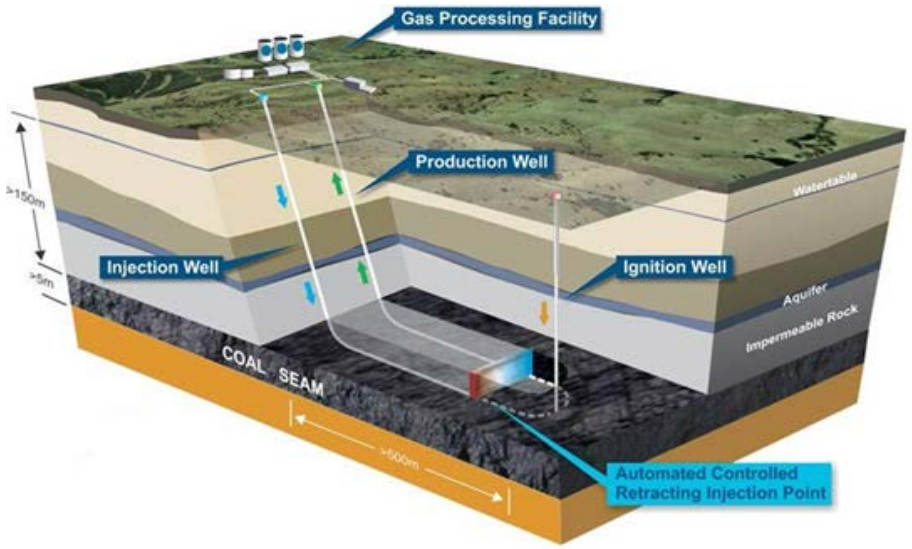

Figure-1 : UCG process with Controlled Retracting Injection Point (CRIP) method for keyseam® [6]

A typical UCG operation using CRIP method is presented in the Figure -1.*Carbon Energy*, *Australia* developed and validated their proprietary UCG technology keyseam® UCG , through joint venture program with Commonwealth Scientific and Industrial Research Organization (CSIRO), Australia, for 10 years of research and 5 years of in-field trials & development. They have successfully demonstrated the keyseam® UCG technology by proving automation

of its *Controlled Retractable Injection Point (CRIP)* technology. Another propriety technique is εUCG™, developed by Ergo Exergy Technologies Inc. (Ergo Exergy) of Canada. *Single Well Flow Tubing (SWIFT)* technology, developed by Portman Energy, is another technological development, where a single vertical well used for both injecting oxidants and delivery of Syngas [7].

The Angren UCG facilities (currently belongs to Uzbekistan) is the only running plant since 1960; but their practice and procedures are not up to the mark [8]. North America, EU, China, Russia conducted joint venture feasibility study with the research organizations. Australian state government funded UCG program (Carbon Energy and CSIRO at Dalby, 5MW Power Station) was a great initiatives for standard practices. Another successful operation of Chinchilla pilot project is treated as western world's ground breaking achievement in UCG for controlling process & shut down practices as well as validation of numerical results scientifically. A number of tools are available to verify modelled predictions, monitor the UCG process and to detect any changes in the gasification environment such as water influx, less flow of air charge etc. Linc Energy, Australia demonstrated their modern practices in Chinchilla project (with 100% availability, 1999-2002) for integrated power generation program had been run for 12 years , operated 5 successive UCG activity, running of GTL(gas to liquid) plant. But unfortunately UCG industry falls behind the race while Coal Seam Gas (CSG) industry is in booming state and the state government sets up a threshold barrier for further progression of UCG commercial operation in Australia [9, 10].

1.3 UCG Projects Around the Globe

Many countries conducted several attempts and pilot projects for demonstrating their capabilities on UCG operation for controlling the process efficiently and minimizing environmental impact since 1940. USA showed huge interest in 1970's -1980's and Europe, China followed by 1990s. USA government instituted more than 30 research projects and UCG trials (Hanna I, II,III & IV and The Rocky Mountain- I) demonstrated the gasification of about 30,000 tons of coal [2]. Development initiatives and licenses issued to exploit UCG in South Africa, South America, the UK, New Zealand, Vietnam, India, Indonesia and other areas. China conducted number of programs, along with different approach for developing the UCG facilities in the exploited u/g coal miner's goaf areas. The *Thar* project in Pakistan is a huge potential UCG project and they have already achieved capabilities for commercial production [10]. Among the running activities, potential UCG projects are summarized in the Table-2.

Table 2. Current UCG program and activities around the Globe

Country		UCG Activity
USA		Lawrence Livermore recently conducted two large projects in Washington and Wyoming and their Cook Inlet project in Alaska is going to commercial production in 2015.
Canada	:	• Swan Hills Synfuels ltd. is developing deep seated UCG operation, Alberta, Canada. • Laurus Energy (technology provider Ergo Exergy) received permit UCG project in Parkland County, Alberta. Ergo Exergy's propriety εUCG™ Technology and expertise was also recognized by Canadian regulators, offering them the appropriate confidence to permit this project for Canada. • Clean Coal Ltd.(UK) and Stealth Ventures Ltd. working in Nova Scotia UCG project.
Chile	:	Carbon Energy, Australia and Antofagasta Minerals jointly working for developing UCG project in Mulpun.
Argentina	:	Carbon Energy, Australia and Delmo Group ltd. going on join venture commercial scale UCG

Country		UCG Activity
		project. Carbon Energy is providing keyseam® technology and related services.
Uzbekistan	:	Linc Energy and Yerostigaz joint venture UCG operation producing about 1 million cubic meters (35 m cft.) of syngas per day in Angren. This is only running plant since 1960.
South Africa	:	Eskom Holdings ltd , Ergo Energy and Sasol New Energy ltd. are collectively working in Mojuba UCG plant. Ergo Exergy's proprietary εUCG™ technology is adopted for UCG operation to generate apx.1,200 MWe of electricity. Their commercial operation will start soon.
European Union	:	• Wild horse Energy conducting the most advanced European UCG program in Hungary. • German UCG Research Program ; EU funded deep seated UCG program with carbon capture, Aachen University, DM, Germany. • Spanish Trial Pilot Project ; EU funded trial finished in 1998, R & D continues.
Australia-New-Zealand	:	• Cougar Energy, Linc Energy and Carbon Energy(join venture with CSIRO), Australia are the renowned UCG technology provider in global context. They had successfully conducted the pilot programs in Kingaroy, Chinchilla and Bloodwood creek projects. However their program is stalling due to booming of CSG operation. • Ergo Exergy and Solid Energy conducted pre-feasibility studies of the Huntly coal field of North Island, New Zealand. Ergo Exergy's proprietary εUCG™ technology is adopted for UCG pilot program to deliver approximately 5,000Nm3/hr for research & development purpose.
China	:	• Zhengzhou Coal Industry Group Co Ltd and Carbon Energy, Australia; under taken a join venture UCG project in Inner Mongolia, China. • ENN group conducted pilot project and planning for expansion of UCG project.
Pakistan	:	Cougar Energy is developing the Thar project in Pakistan since 2007 adopting the Ergo Exergy's proprietary εUCG™ technology for 100 MW electricity generation.
India	:	Abhijeet, India, AE Coal Technologies Ltd making efforts to obtain the block for conducting it's first εUCG™ development in the Kaitha coal block situated in Ramgarh district.
Vietnam	:	Link Energy, Australia; is working in Vietnam in Red River Delta project (included 2 projects) for developing the capabilities for further commercial development.
Indonesia	:	Carbon Energy, Australia is working in Indonesia for developing the capabilities for further commercial development.
Bangladesh	:	• Abhijeet Group, Indian, Silicon Tech, has proposed to develop UCG facilities in the Jamalganj coal mine in Joypurhat and to install a power plant under a joint venture with Petrobangla[11] . • Clean Coal Limited, USA proposed to produce 5,000 megawatts power by using underground coal gasification (UCG) technology at Jamalganj [12].

1.4Why Should Bangladesh Step Ahead for Developing UCG Project?

It is recognized in global perspectives that UCG is economically viable and a sustainable engineering approach for *Integrated Gasification Combined Cycle (IGCC)* power generation. Barapukuria Coal Mine operation was interrupted from technical problems and surface subsidence. Further extraction of long wall slices would be more difficult with obvious subsidence. An alternative study conducted on Barapukuria coal mine for further provision of open pit mining. But water modelling prediction suggested for dewatering of 344 million m^3 of incoming water and subsequent water management program [13]. This water hazard may be out of control in the rainy season. Considering these hazardous factors, it is very difficult to stepping for further open pit mining. The discovered coal reserves and their present status can be found in the following Table-3.

Table 3. Major coal fields and reserves in Bangladesh

Coal field	Thickness (av.), m	Depths of coal seam (m)	No. of coal seam	Reserve (m. ton)	Status
Jamalganj *(Kuchma ,Bogra)*	64.0 m	640-1158	7	1053	Mining not feasible economically
Barapukuria *(Dinajpur)*	51.0 m	118-506	6	303	Underground mine started production
Khalaspir *(Rangpur)*	50.0 m	257-451	8	147	Undeveloped
Dighipara *(Dinajpur)*	61.0 m	250	7	200	Undeveloped
Phulbari *(Dinajpur)*	38.4 m	152-246	1	380	Open pit mine feasibility study undertaken in 2004

Two other coal-bearing basins are known (Nawabgonj and Dangapara), but have undefined reserves. Four coal reserves (Badargonj, Osmanpur, Burirdoba and Shimnagar) in Gondwana basins have been identified but are not yet known to host coal measures. The geological condition, depth of deposit, environment and ecological impacts in respect of return and cost effective operation are considered for choosing coal extraction method. The unconventional methods for exploiting coal energy as : (1) Coal Seam Gas (CSG) / Coal Bed Methane (CBM) operation, (2) Underground Coal Gasification (UCG), (3) Biotechnology in coal reserve (R & D stage), (4) Borehole Mining (research stage) etc. Among other unconventional coal extraction method, UCG can be chosen as alternative energy extraction method for above coal deposits. Coupling of gasification process to power generation, especially deep seated coal seams of Jamalganj, where environmental issues like the ground water contamination, subsidence can be omitted/ minimized.

1.5 Potential Environmental Issues on Water, Land Surface Subsidence

UCG is treated as clean coal technology and best practicing of UCG technology can be the cleanest coal usage for power generation which will keep the minimum level of deadly Sulphur and Nitrogen oxides, GHG emission, solid waste etc. This can be achieved through implementation of best practices and sophisticated engineering for process control and operational efficiency. The gasification cavities of the coal seams are sources of gaseous and liquid

pollutants and they constitute some environmental risks to groundwater in the adjacent strata. Deeper seams are less likely to be linked with aquifers and reduced probability of contamination with pyrolysis products. The EU are working on exploiting their deep seated coal deposits in a composite manner like Integrated Coal Gasification - Combined Cycle Power Plant and post Carbon Capture & Storage within in-situ coal cavity, which is modelled as optimization of coal resources. The physic-chemical interactions of UCG process changes the natural stress state in the surrounding rock mass, influencing in contaminants formations in the UCG reactor and through the surrounding ground, as well as inducing potential subsidence and pollutions of the groundwater, surface water. Subsidence is a major problem for shallow depth coal gasification activity , which decreases with increasing of depth.

1.6 The Regulations Around the World Regarding UCG Development

For commercialization of UCG, the legislative issues needed to be addressed properly. Regulatory issues became a vital factor for some of the UCG projects hampered by a lack of suitable regulations such as Pakistan, South Africa, where legislation and permitting for UCG is not catered for in existing acts and legislation. On the other hand in Alberta, Canada where a good regulatory framework exists for ISCG (in-situ coal gasification) or UCG is provided by the Energy Resources Conservation Board (ERCB) of Alberta. The pilot project is completed and are planning to establish a commercial project. In Australia the Queensland state government had formed an Independent Scientific Panel for further steps on commercial UCG operation. That technical committee also recommended for establishing two new entities for supporting the UCG industry as: (1) Queensland UCG Independent Assessment, Evaluation and Advisory Group and (2) The Queensland UCG R&D Network.

2. Identified Issues for Stepping to UCG

An independent technical review on " Coal-bed Methane (CBM) and Underground Coal Gasification (UCG) potential in Bangladesh" conducted by mining geologist Mark Muller, presented a real life facts figure about coal energy in 2009, but situation remained unchanged till dated[14]. Bangladesh is planning for constructing coal based power station running with imported coal, whereas extraction of the own coal resource remain a neglected option. In the USA, most of the pilot projects and studies were conducted jointly with U.S Department of Energy and Lawrence Livermore National Laboratory are hatching the technological development for global perspectives. Before opening the chapter for UCG development with the help of global organization, Bangladesh must have to do homework on their own resources for achieving bargaining capacity with facts figure within the expert groups.

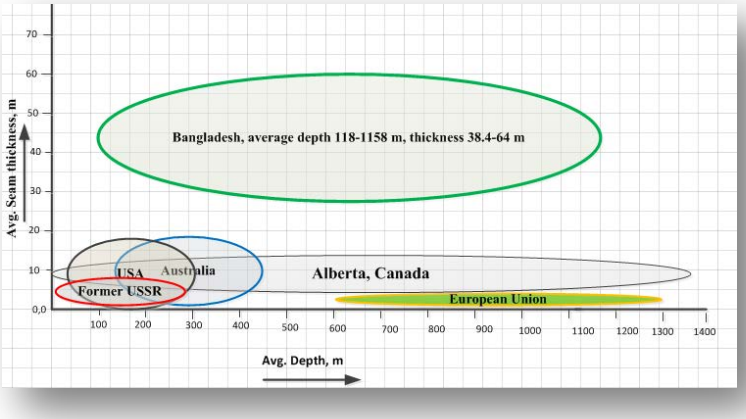

Figure-2: Comparative presentation of UCG coal seams targeted for global perspectives

The scenario for coal deposits in Bangladesh is quite different from other areas. It is presented in the Figure-2 in respect of mean thickness and position below the surface level. It is needed to extensive study and research through numerical modelling, laboratory simulations considering the identified issues mainly (i) Thickness of the coal seam, (ii) Bituminous Coal, (iii) Long column of water bearing aquifer, (iv) Strength & Hardness of the host/cap rock, (v) Surface subsidence , (v) Purpose of usages and choosing of operational method etc. Bangladesh may take initiatives for developing UCG within the framework of one pilot project for achieving competency in the identified issues as follows.

2.1 Bird's Eye View on Coal Geology of Bangladesh

Coal is a sedimentary rock composed of lithified plant materials, with small amount of inorganic impurities, (formed 100-400 Million years ago) and their quality depends on the formation process, temperature, pressure as well as materials, where geological condition plays the main role. Geological formation of the overburden is the main consideration for further progression of UCG activity in Bangladesh. The geological evolution of Bangladesh is mainly related to uplift of the Himalayan Mountains, rapid subsidence and sinking, evolution of sedimentary basins through formation of the Bengal delta. The Permian sediments in most parts of the world are rich in coal because of the favorable coal forming condition. The Gondwana Group of Permian age is the oldest sedimentary unit in Bangladesh. It rests un-conformably on the Precambrian Crystalline basement. The Gondwana Group is composed of hard sandstone with some inhibited coal and shale layers. The Group is about 1000m thick and is found in fault bounded Graben basins. Major bituminous coal deposits are located in Rangpur and Dinajpur districts because of the occurrence of Permian Sediments in the fault bounded graben basin above the Precambrian basement. The evolution and formation of the basins (having coal deposits) can be understand through study on Plate Tectonic Theory. The tectonic map of Bangladesh is divided into two major tectonic units and a minor transition zones as: (1) Stable Pre-Cambrian Platform ,(2) Geosynclinal basin and (3) Palaeo continental slope called the hinge zone. The general structure of the fault geometry can be described as Horts-Saddle-Graben in the Figure-3. Bogra Shelf, a part of the Stable Pre-Cambrian platform, represents the southern slope of the Rangpur Saddle. The width of Bogra Shelf varies from 60-125 km up to the Hinge Zone and the thickness of the overlying sedimentary sequence increases towards the southeast. It is a regional monocline plunging gently southeast towards the Hinge Zone [16].The Bengal Basin contain Permian age sedimentary rocks like as Gondwana, Rajmahal, Tura, Jaintia and Surma Groups, Dupi Tila and Madhupur Clay Formations lying over the basement. The sedimentary rocks are found as 120 m to 3000m thick above the Pre-Cambrian platform region which includes Rajshahi, Bogra, Rangpur and Dinajpur areas. It is sub-divided into (i) Northern Rangpur Saddle with a very shallow Precambrian basement (130 to 1,000m) and (ii) Southern Bogra Shelf with a Basement at moderate depth (1 to 6 km).

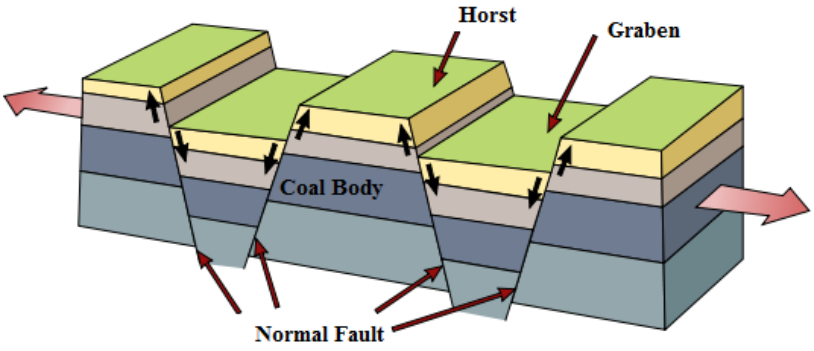

Figure-3 : General structure of the Fault Geometry of NW Bangladesh[15]

In the Rangpur Saddle the basement is uplifted and is covered with thin sedimentary deposits. Maddhapara Granite Mine (adjacent to Barapukuria Coal Mine) falls in this area where the basement is only 130m below the ground surface. It is overlain by sedimentary rocks of Plio-Pliestocene age like as Dupi Tila Sandstone and Madhupur Clay. The top of the basement at the Rangpur Saddle exhibits a good degree of flatness and slopes in all directions. The basement has suffered intense faulting [17].

2.2 Structural Integrity of Capping Rock

Host rock and coal can be created through same sort of geological forces. The coal deposits may overlain by permeable sedimentary rock formation. However the faults and discontinuity in the coal seam can provoke linkage of aquifer to the UCG cavities. Tectonic activity can create faults and fractures through which UCG gas may escape or water inflow towards reaction zone. High temperature cause thermal stresses and shrinkage, introduces crack/fractures, later on collapse of the burn cavity.

An exclusive study conducted for rock mass classification in stopes by Extension Fuzzy Method (EFM) in Maddhapara Granite Mine, for estimating Pillar strength considering uni-axial compressive strength of rock with multiplication factor. The Numerical Modelling is conducted using Finite Element simulation package FLAC 2D/3D. The Geological stratigraphy of Maddhapara Hard Rock Mine (close vicinity to the coal basins) confirmed through borehole geological survey that the basement is covered with the several formations such as Alluvium, Madhupur clay, Dupitila Formation, Tura Formation, Gondwana, Kaoline, Weathered Rock etc. Among them Madhupur clay, Kaoline, both are assumed to be impermeable layer. The UCG cavity experiences stress changes due to induced stress redistribution as the cavity increases in size and Stress effects due to the thermal response of rocks surrounding the cavity. The UCG cavities roof collapse and subsequent development of subsidence is influenced by the strength of rocks overlying the coal seam.

2.3 Rainfall and Recharging of Flood water to Aquifer

The rainfall in Bangladesh depending upon season and location varies from 1500 mm in the west-central part to over 3000 mm in the northeast and southeast. The rainy season (June -October) accounts for 70 to 85% of the annual rainfall. Almost one-third of the land area of Bangladesh is covered by normal flood and severe flood covers more than half of the country. From upstream, surface water flows towards Bay of Bengal, seeped down, accumulates in porous strata and underground sub-soil structure in rock layers called “aquifer”.

Aquifer is a geological group-formations and groundwater reservoirs. The aquifer system generally consists of three lithological units as; (1) an upper silty clay and silt layer called the Composite Aquifer, usually 30 to 60 m thick, (2) a middle layer of fine to very fine sand called the Main Aquifer about 20 m thick, and (3) a lower layer of fine to coarse sand constituting the Deep Aquifer, is about 100 m thick. The water table varied with season and normally found close to ground surface. The Deep Aquifer is separated from the overlying main aquifer by one or more clay layers of different thickness[18]. UCG operation having a potential risk of contamination/acidification of groundwater by the product gases as they pass upwards through production well failure or groundwater interacts with the combustion chamber, leaching toxic materials such as phenol and benzene. Through proper site selection and operation management, these aquifer contamination can be minimized through optimistic *Triple Lock Mechanism* as Hydrodynamic Trapping, Pressure-Arch Trapping, Geochemical Trapping as presented in the Figure-4 [19,20,21,22].The water modelling for the UCG sites should be done with hydrodynamic property. Detailed study and water modelling documents of Bangladesh are available in respective department.

2.4 Surface Subsidence Studies Relating to UCG Activity

The cavity growth more or less circular for low thickness seam, but it is Spherical or Ovaloid shaped for thick seams. UCG operations creates the same nature of surface subsidence like the underground mining but the size and

degree of collapse mainly administered by the mechanical strength of the overlying rocks and their properties . The collapse of UCG cavities can result in possible contamination of deep aquifers. The degree of severity of surface subsidence depends on cavity size and supporting pillar size of the coal body. As the thickness of the coal seams are very high and quiet different from global perspectives. Extensive study should be conducted through Numerical Modelling and simulation considering the coal seam dimension, overlaying capping rock strata.

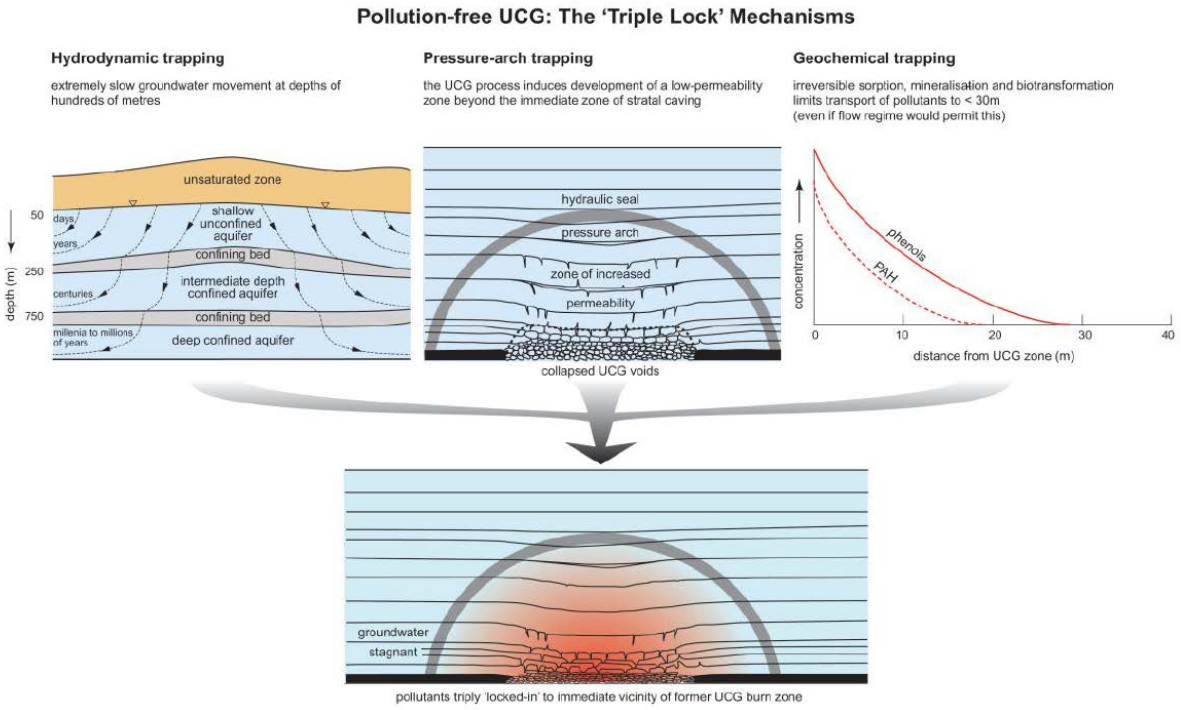

Figure-4: 'Triple Lock' Mechanism of UCG [21]

2.5 Bituminous Coal

The discovered coal reserves are mainly Bituminous/ sub-Bituminous high grade coal. Mathematical model calculation shows that the heating value of gas produced from either lignite or bituminous coal should be lower than the heating value of gas from sub-bituminous coal. Bituminous coal contains less volatile matter and therefore, produces a lower heating value gas. This is a vital issue for design criteria of UCG development.

2.6 Choosing of Operational Methods, CFD modelling and Analysis of UCG Gasification Process considering Hydrological and Geological conditions

Mainly two aspects are considered for modelling of UCG processes as; (1) Temperature & pressure profiles and (2) Cavity growth, subsidence and other mechanical aspects. The combustion gases flow through the coal bodies providing environment of endothermic steam-char reaction for producing the combustible gas. The advancement of flame propagation and cavity growth is the prime objectives for efficient coal energy recovery. It is also related to

support pillar calculation, roof collapse, water influx, groundwater contamination, surface subsidence and other issues. Considering the ideal cases and influencing factors, the developed numerical models and mathematical results were found close matching with the experimental results and real life field test [23-25]. UCG involves intimate-coupled multi-physical/chemical processes, occurred in different areas, such as UCG cavity, the deforming of coal body, spalling of coal, porous wall zone and the rubble zone, with the thermal-hydrological-geo-mechanical processes, water influx, roof collapse, subsidence etc. For detailed study of the UCG cavity growth, Lawrence Livermore National Laboratory, USA are developing the 3D UCG simulator (a project sponsored by USA government) base on the modelling approach developed by Britten and Thorsness [26-27]. The model predicts decline rates of cavity surfaces and generation rates of major product species that compare well with experimental data from two UCG field tests[4]. The numerical models are capable of predicting the outcomes. The basic model components for the simulation approach contain the following area as presented in the Figure-5 as:

- Geo-mechanical Model (Roof collapse, Subsidence, Stress Changes & Fracturing),
- Boundary Evolution Model (cavity Growth from wall reactions & Structural failure, Rubble Zone Geometry, Roof Movement due to Structural failure),
- Wall Zone Model (Reaction & drying, Heat & Mass Transport, Spallation, Gas & Solid Compositions),
- Rubble Zone Model (Reactions & Drying, Heat & Mass Transport, Gas & Solid Compositions),
- Thermal-Hydrological Model (Groundwater Flow & Influx, Pore Pressure Field, Thermal Response),
- Cavity Gas Model (Reactions & Gas Composition, Heat & Mass Transport, Turbulent Mixing),

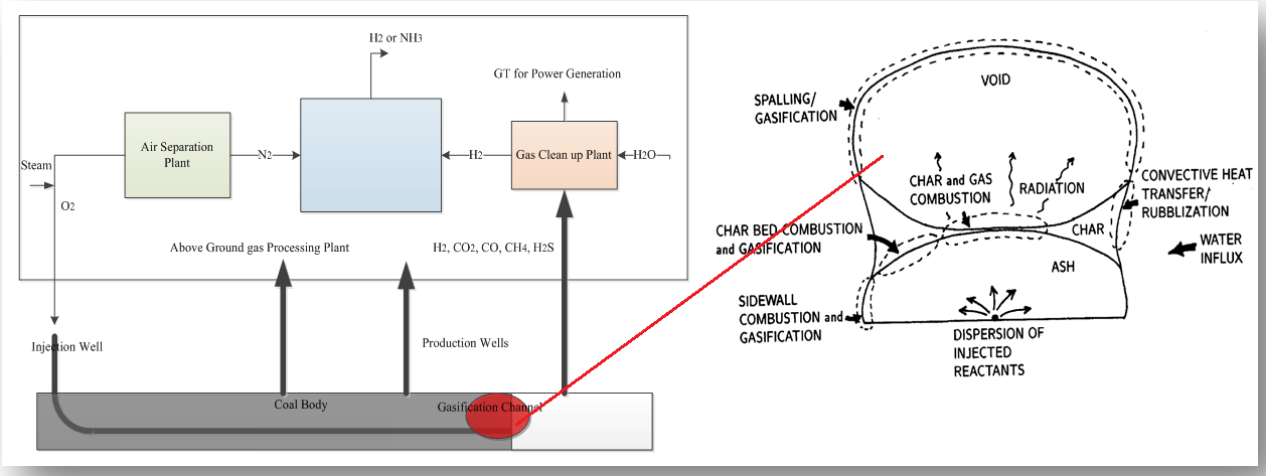

Figure 5: Schematic Diagram of Above ground Gas processing facilities and UCG Cavity Growth process [4]

3. Concluding Remarks and Further Works

UCG categorized as an extreme energy process because of its unpredictable operational state, but the experts around the globe are claiming that they are ready for harnessing the challenges of this Black Beauty. Controlling of physical and chemical mechanisms occurs at UCG are being successfully demonstrated with instrumented laboratory experiments. Research organizations /Universities are conducting projects & studies funded by government agencies and private business groups. In return the scientist group and experts successfully pointed out the relevant issues and their possible solution through Numerical modelling, computer simulation and validated in UCG simulator facilities in the laboratory along with real life pilot projects. UCG is already been accepted as a proven clean coal technology, but selection of best technological procedure is a variable function depending on real life factors. Bangladesh should raise their facts figure and find out the problems and issues. Later on seeks for solutions through reliable engineering design and practices for combating obstacles for commercial operation of coal gasification.

Two critical problems are identified as major setbacks for implementation of the UCG in Bangladesh as land subsidence and water inflow/influx. Finite Element study in ABAQUS environment would be conducted for further analysis. A 3D thermal-mechanical modelling around UCG cavities can be simulate using the computational software ABAQUS. The model would be able to simulate the heat propagation, stress distribution and surface subsidence in UCG process. Another model would be developed in ANSYS environment for CFD (computational fluid dynamics) analysis to investigate the effect of various parameters on the UCG process.

4. References

1. Burton, E., J. Friedmann, and R. Upadhye, Best Practices in Underground Coal Gasification. Lawrence Livermore National Laboratory, USA.
2. Klimenko, A.Y., Early Ideas in Underground Coal Gasification and Their Evolution. Energies, 2009. 2: p. 456-476.
3. Markus, B. and e. al Syngas Production from Coal. ETSAP Energy Technology Systems Analysis Programme, 2010.
4. Shafirovich, E. and A. Varma, UCG: a brief review of current status. Ind. Eng. Chem. Res., 2009. 48,: p. 7865–7875.
5. Upadhye, R., E. Burton, and J. Friedmann, Science and Technology gaps in Underground Coal Gasification. 2006, US Department of Energy , University of California, Lawrence Livermore.
6. www.carbonenergy.org. Underground Coal Gasification Keyseam™, 2014.
7. Kumar, H., et al., Underground Coal Gasification: an alternate, Economical, and Viable Solution for future Sustainability. International Journal of Engineering Science Invention, 2014. 3(1): PP.56-67.
8. Green, M. Underground Coal Gasification, State of the Art. in Clean Coal Conferance'2008. Bedewo, Poland.
9. Moran, C., J. Costa, and C. Cuff, Independent Scientific Panel Report on Underground Coal Gasification Pilot Trials. 2013, Queensland Independent Scientific Panel for Underground Coal Gasification (ISP): Queensland, Australia.
10. Ghose, M.K. and B. Paul, Underground Coal Gasification: a Neglected Option. International Journal of Environmental Studies, 2007. 64:6: p. 777-783.
11. www.ucgassociation.org/index.php/news/archives/200_. Bangladesh Project Plan. 2014.
12. http://www.sourcewatch.org/index.php. Bangladesh and Coal. 2011.
13. www.energybangla.com/index.php.
14. Muller, M. Coal-bed Methane (CBM) and Underground Coal Gasification (UCG) potential in Bangladesh. 2009; Available from: http://www.minesandcommunities.org.
15. www.wikipedia.org/wiki/Graben. Graben. 2014.
16. Chowdhury, S.Q., Pre-Cambrian Indian Platform, Banglapedia. http://www.banglapedia.org ,2012.

17. Guha, D., Stable Pre-Cambrian Platform, Banglapedia. http://www.banglapedia.org , 2012.
18. Hossain, M.S., Aquifar, Banglapedia. http://www.banglapedia.org/english/index/H.htm. 2012.
19. Jarral, M., Underground Coal Gasification and Power generation; Health, Safety and Environment Aspects. 45th. IEP Convention, 2012. The Institution of Engineers Pakistan. Karachi Centre.
20. Younger, Paul L., Hydrogeological and Geo-mechanical Aspects of Underground Coal Gasification and its Direct Coupling to carbon Capture and Storage. Springer-Verlag, 2011, 10.1007/s10230-011-0145-5.
21. Roddy, Dermot "Five Quarter : Clean Syngas from Under the Seabed" , Five Quarter Energy Holdings Ltd. www.five-quarter.com
22. Younger, Paul L., "Unconventional Exploitation and the Environment" University of Glasgow, UK.
23. Yang, L., Numerical Study on the Underground Coal Gasification for Inclined Seams. Environmental and Energy Engineering, 2005. 51.
24. Yang, L.H., A Review of the Factors Influencing the Physicochemical Characteristics of Underground Coal Gasification. Energy Sources,:, 2008. Part A(Recovery, Utilization, and Environmental Effects).
25. Biezen, E.N.J., J. Bruining, and J. Molenaar, "An Integrated 3D Model for Underground Coal Gasification", in Society of Petroleum Engineers Annual Conference. 1995: Dallas, USA.
26. John J. Nitao, et al., Progress on a New Integrated 3-D UCG Simulator and its Initial Application, in International Pittsburgh Coal Conference. 2011: Pittsburgh, PA, United States.
27. Britten, J.A. and C.B. Thorsness, A Model for Cavity Growth and Resource Recovery during Underground Coal Gasification. In Situ 1989,. 13, p. 1–53.

…….